



## The potential anti-Alzheimer's activity of *Oxalis corniculata* Linn. Methanolic extract in experimental rats: Role of APOE4/LRP1, TLR4/NF- $\kappa$ B/NLRP3, Wnt 3/ $\beta$ -catenin/GSK-3 $\beta$ , autophagy and apoptotic cues

Karema Abu-Elfotuh<sup>a,b</sup>, Ahmed M.E. Hamdan<sup>c,\*</sup>, Shaza A. Mohamed<sup>d</sup>, Riham O. Bakr<sup>e</sup>, Amal H. Ahmed<sup>d</sup>, Ahmed M. Atwa<sup>f</sup>, Amira M. Hamdan<sup>g</sup>, Ahad Ghanem Alanzai<sup>h</sup>, Raghad Khalid Alnahhas<sup>h</sup>, Ayah M.H. Gowifel<sup>i</sup>, Maha A. Salem<sup>i</sup>

<sup>a</sup> Clinical Pharmacy Department, Faculty of Pharmacy (Girls), Al-Azhar University, Cairo, Egypt

<sup>b</sup> Al-Ayen Iraqi University, Thi-Qar, 64001, Iraq

<sup>c</sup> Pharmacy Practice Department, Faculty of Pharmacy, University of Tabuk, Tabuk 74191, Saudi Arabia

<sup>d</sup> Pharmacognosy and Medicinal Plants Department, Faculty of Pharmacy (Girls), Al-Azhar University, Cairo 11754, Egypt

<sup>e</sup> Department of Pharmacognosy, Faculty of Pharmacy, October University for Modern Sciences and Arts (MSA) University, Giza 11787, Egypt

<sup>f</sup> Pharmacology and Toxicology Department, Faculty of Pharmacy, Egyptian Russian University, Badr City, Cairo-Suez Road, Cairo 11829, Egypt

<sup>g</sup> Oceanography Department, Faculty of Science, Alexandria University, Alexandria 21511, Egypt

<sup>h</sup> Faculty of Pharmacy, University of Tabuk, Tabuk 74191, Saudi Arabia

<sup>i</sup> Pharmacology and Toxicology Department, Faculty of Pharmacy, Modern University for Technology and Information (MTI), Cairo 11571, Egypt

### ARTICLE INFO

Handling Editor: Dr. Thomas Efferth

#### Keywords:

Alzheimer's disease  
*Oxalis corniculata* Linn  
Oxidative stress  
Autophagy  
TLR4/NF- $\kappa$ B/NLRP3  
Wnt 3/ $\beta$ -catenin/GSK-3 $\beta$   
PERK/CHOP/Bcl-2  
APOE4/LRP1

### ABSTRACT

**Ethnopharmacological relevance:** *Oxalis corniculata* (*O. corniculata*) is a member of Oxalidaceae family, widely distributed in Asia, Europe, America, and Africa, used extensively as food and its traditional folkloric uses include management of epilepsy, gastric disorders, and neurodegenerative diseases, together with its use in enhancing health. Numerous pharmacological benefits of *O. corniculata* are linked to its anti-inflammatory and antioxidant abilities. One of the most prevalent neurodegenerative disorders is Alzheimer's disease (AD) in which neuro-inflammation and oxidative stress are its main pathogenic processes.

**Aim of the study:** Our research aimed to study the neuroprotective effect of the methanolic extract of *Oxalis corniculata* Linn. (*O. corniculata* ME), compared to selenium (Se) against AlCl<sub>3</sub>-induced AD.

**Materials and methods:** Forty male albino rats were allocated into four groups (Gps). Gp I a control group, the rest of the animals received AlCl<sub>3</sub> (Gp II-Gp IV). Rats in Gp III and IV were treated with Se and *O. corniculata* ME, respectively.

**Results:** The chemical profile of *O. corniculata* ME was studied using ultraperformance liquid chromatography-electrospray ionization-quadrupole time-of-flight mass spectrometry, allowing the tentative identification of sixty-six compounds, including organic acids, phenolics and others, cinnamic acid and its derivatives, fatty acids, and flavonoids. AlCl<sub>3</sub> showed deterioration in short-term memory and brain histological pictures. Our findings showed that *O. corniculata* ME and selenium helped to combat oxidative stress produced by accumulation of AlCl<sub>3</sub> in the brain and in prophylaxis against AD. Thus, Selenium (Se) and *O. corniculata* ME restored antioxidant defense, via enhancing Nrf2/HO-1 hub, hampered neuroinflammation, via TLR4/NF- $\kappa$ B/NLRP3, along with dampening apoptosis, A $\beta$  generation, tau hyperphosphorylation, BACE1, ApoE4 and LRP1 levels. Treatments also promoted autophagy and modulated Wnt 3/ $\beta$ -catenin/GSK3 $\beta$  cue.

**Conclusions:** It was noted that *O. corniculata* ME showed a notable ameliorative effect compared to Se on Nrf2/HO-1, TLR4/NF- $\kappa$ B/NLRP3, APOE4/LRP1, Wnt 3/ $\beta$ -catenin/GSK-3 $\beta$  and PERK axes.

\* Corresponding author. Department of Pharmacy Practice, Faculty of Pharmacy, University of Tabuk, P.O Box: 741, Postal Code: 71491. Saudi Arabia.

E-mail addresses: [Karimasoliman.pharmg@azhar.edu.eg](mailto:Karimasoliman.pharmg@azhar.edu.eg) (K. Abu-Elfotuh), [a\\_hamdan@ut.edu.sa](mailto:a_hamdan@ut.edu.sa) (A.M.E. Hamdan), [shazahalim2652.el@azhar.edu.eg](mailto:shazahalim2652.el@azhar.edu.eg), [shaza.halim@hotmail.com](mailto:shaza.halim@hotmail.com) (S.A. Mohamed), [romar@msa.edu.eg](mailto:romar@msa.edu.eg) (R.O. Bakr), [amalhussain.52@azhar.edu.eg](mailto:amalhussain.52@azhar.edu.eg) (A.H. Ahmed), [ahmed-atwa@eru.edu.eg](mailto:ahmed-atwa@eru.edu.eg) (A.M. Atwa), [Amirahamdan@alexu.edu.eg](mailto:Amirahamdan@alexu.edu.eg) (A.M. Hamdan), [ahdgh9791@gmail.com](mailto:ahdgh9791@gmail.com) (A.G. Alanzai), [Raghadk2alid@gmail.com](mailto:Raghadk2alid@gmail.com) (R.K. Alnahhas), [ayah.gowifel@pharm.mti.edu.eg](mailto:ayah.gowifel@pharm.mti.edu.eg) (A.M.H. Gowifel), [Maha.Salem@pharm.mti.edu.eg](mailto:Maha.Salem@pharm.mti.edu.eg) (M.A. Salem).

<https://doi.org/10.1016/j.jep.2024.117731>

Received 13 October 2023; Received in revised form 23 December 2023; Accepted 6 January 2024

Available online 11 January 2024

0378-8741/© 2024 The Authors. Published by Elsevier B.V. This is an open access article under the CC BY-NC-ND license (<http://creativecommons.org/licenses/by-nc-nd/4.0/>).

## 1. Introduction

Worldwide, there are around fourth million individuals suffering from Alzheimer's disease (AD), the most common neurodegenerative disease of ageing, but there are currently few effective treatments (Jeremic et al., 2021). By 2050, this figure is expected to exceed 130 million (Cano et al., 2021). Patients with AD suffer from short-term memory loss, which makes it hard to carry through their daily duties efficiently and successfully (Ahmad and Sachdeva, 2022). The causes of the pathological alterations in AD are still unclear. The neuropathological alterations in AD are categorized into two features, beta-amyloid protein (A $\beta$ ) extracellular deposits (Breijyeh and Karaman, 2020) and Neurofibrillary Tangles (NFT), which are atypical threads of hyperphosphorylated tau protein (Verde, 2022). The accumulation of A $\beta$  is thought to alter cholinergic neurotransmission, leading to a reduction in the release of acetyl choline (Ach) (Giacobini et al., 2022). In addition, other theories proclaim that inflammation exerts a key part in the etiopathology of AD (Mohamed et al., 2021). Moreover, robust levels of reactive oxygen species (ROS) relate to the etiopathology of AD (Vilalpando-Rodriguez and Gibson, 2021). In fact, overexposure to aluminum (Al) results in the initiation and progression of numerous neurodegenerative disorders, including AD, where aluminum boosts oxidative stress, encourages the cross-linking and deposition of A $\beta$ , together with the development of plaques in the brain, hence these features mimic those occurring in pathology of AD in humans (ELBini-Dhouib et al., 2021; Mehrbeheshi et al., 2022). Besides, the pervasiveness of aluminum (Al) in the environment, daily life activities and food makes the exposure to aluminum unavoidable. Therefore, aluminum chloride (AlCl<sub>3</sub>)-induced AD in rodents is recognized as a reliable model for studying the neuroprotective effects of many natural and synthetic compounds against AD (Skalny et al., 2021). In the context of pharmacological intervention, the current therapies for AD are not capable of halting the progression of the illness. However, these agents offer moderate benefits since they help in reducing symptoms (Sharifi-Rad et al., 2022b). Chronic inflammation and oxidative stress (OS) impose the prompt application of novel therapies with improved effectiveness against AD and reduced side effects. Shortcomings in the available treatments for AD highlight the need to find novel sources of chemicals with potent anti-degenerative properties to prevent the acute neurological decline brought on by the disease. Hence, finding neuroprotective bioactive components that are efficient in preventing, and curing AD while being devoid of negative side effects for patients is now essential. Considering the latter, natural substances are promising as supplemental and alternative treatments for neurodegenerative illnesses (Sharifi-Rad et al., 2022a,b; Welcome, 2020). Phytochemicals are bioactive secondary metabolites, which include alkaloids, polyphenols, terpenoids, organosulfur compounds, limonoids, furyl compounds, polyenes, thiophenes, peptides, saponins, sterols, lignans, tannins, and stilbenes (Hossain et al., 2022a, 2022b).

Selenium (Se) plays a substantial part in cellular processes, including detoxification, controlling redox balance, and immunity. Multiple studies were conducted to investigate the beneficial values of Se in neurodegenerative maladies, like AD. Se was found to have the ability to prevent the synthesis of amyloid beta fibers (A $\beta$ ) and break down already-formed A $\beta$  fibers into harmless aggregates in addition to decreasing hyperphosphorylation of tau protein and preventing neuronal death (Lakshmi et al., 2015). Moreover, Se levels are linked to altered neurotransmitter metabolism. However, Se's antioxidant activity may be the most crucial role in AD (Gao et al., 2020).

*Oxalis corniculata* (*O. corniculata*) is a member of Oxalidaceae family, extensively dispersed in Asia, Europe, America, and Africa (Li et al., 2006). It is abundantly growing along roadsides, in gardens, and in yard. *O. corniculata* is a herbaceous plant that typically thrives in wet, dark environments. The plant contains vital phytochemicals that are necessary for regular and excellent health of human beings. The leaves of *O. corniculata* are quite edible with a tangy taste, where this plant is used

as a good appetizer and recognized for its medicinal value (Li et al., 2006). The traditional uses of *Oxalis corniculata* in folk medicine comprise its use for a variety of health benefits including its use in treatment of neurological disorders like epilepsy, depression, dementia and neurodegenerative maladies (Aruna et al., 2016; Senthil Kumar, 2010; Das and Gohain, 2018a, 2018b); gastric disorders; liver disorders; diabetes; along with its use as anthelmintic; anti-inflammatory; anti-bacterial; diuretic (Mushir et al., 2015; Jain et al., 2023) and in wound-healing (Sharma and Kumari, 2014; Taranalli et al., 2004). In addition, it demonstrated promising beneficial activities as anti-neurodegenerative (Silalahi, 2022), anti-diabetic (Al-Qalhati et al., 2016), cardioprotective (Abhilash et al., 2011), antifungal (Mukherjee et al., 2013), anti-inflammatory (Dighe et al., 2016), as well as antioxidant effects, where it scavenges ROS with enhancing the antioxidant defense mechanisms (Jain et al., 2023). In this plant, both the stem, as well as the bark are utilized in the management of snakebite and bronchitis, whereas juice of the leaves is used as diuretic, digestive agent and in treating dysentery (Gupta et al., 2005; Hukkeri et al., 2006). Those activities are well correlated with a variety of phytoconstituents, including tannins, flavonoids as 6-C-glucosylluteolin (isoorientin), 6-C-glucosylapigenin (isovitexin) and isovitexin 7-methyl ether (Mizokami et al., 2008) in addition to corniculatin A, (luteolin-6''-(E-p-hydroxycinnamoyl) 4'-O- $\beta$ -D-glucopyranoside), luteolin, luteolin-7-O- $\beta$ -D-glucoside, rutin, Kaempferol-3-sophorotrioside, quercetin-3 (caffeoyl di-galactoside)-7-glucoside, isorhamnetin-3-caffeoyl-7-glucoside, other phenolics including hydroxybenzoic, p-coumaric acid, ferulic acid (Ibrahim et al., 2013; Mukherjee et al., 2018; Zeb and Imran, 2019), besides high levels of all-E-violaxanthin, all-E-neoxanthin, all-E-lutein, 9-Z-lutein, and  $\beta$ -sitosterol-3-O- $\beta$ -D-glucoside. Crucial fatty acids like palmitic acid, linoleic acid, linolenic acid, stearic acid, and oleic acid presence have been detected (Khare, 2007). In the light of the traditional uses of *O. corniculata* as a neuroprotective agent against a variety of neurological diseases and neurodegenerative disorders, Aruna et al. (2017), also supported this notion by reporting that *O. corniculata* elicited neuroprotective effects against neurodegenerative diseases, like Parkinson's disease (PD), where it attenuated cognitive and behavioral impairments, improved learning and memory performance in model of PD, via its antioxidant, anti-degenerative, neuroprotective and anti-inflammatory actions, as ROS and neuroinflammation are the main contributors in the pathophysiology of neurodegenerative diseases. Moreover, an in-vitro study depicted notable acetylcholinesterase (AChE) inhibitory activity of the flavonoids isolated from *O. corniculata* (Imran et al., 2020). Noteworthy, isovitexin, one of the constituents of *O. corniculata*, had been reported to exert anti-Alzheimer activities (Herrero and Barja, 2000). Besides, Tillerson et al. (2002) and Tillerson and Miller (2003) reported that the modulatory effect of *O. corniculata* on cholinergic neurotransmission, supported the recommendation of the use of *O. corniculata* as a promising agent in treatment of neurodegenerative maladies, including AD and PD.

In view of the above-mentioned traditional uses and activities, particularly the antioxidant, anti-inflammatory, anti-neurodegenerative, together with the documented neuroprotective activities of *O. corniculata* against neurological disorders, including neurodegenerative maladies, like AD, the aim of this work was designed to inspect the neuroprotective properties of the methanolic extract of *Oxalis corniculata* (*O. corniculata* ME), compared to selenium against AlCl<sub>3</sub>-induced AD, via exploring their impact on Nrf2/HO-1, TLR4/NF- $\kappa$ B/NLRP3, PERK/CHOP/Bcl-2, APOE4/LRP1 and Wnt 3/ $\beta$ -catenin/GSK-3 $\beta$  hubs, the crucial contributors in the pathophysiology of AD. Although *O. corniculata* is used traditionally as neuroprotective agent against wide range of neurological disorders, no such rigorous studies have been conducted yet. Besides, in this study, an in-depth phytochemical profiling for *O. corniculata* entire aerial parts was performed using ultraperformance liquid chromatography-electrospray ionization-quadrupole time-of-flight mass spectrometry (UPLC-ESI-QTOF-MS/MS).

## 2. Materials and methods

### 2.1. Chemicals

Selenium (Se) and aluminum chloride ( $\text{AlCl}_3 \cdot 6\text{H}_2\text{O}$ , CAS Number: 7784-13-6, Product No: 237,078) were procured from Sigma Chemical Co. (St. Louis, MO, USA). Prior to usage, 20 mg  $\text{AlCl}_3$  was dissolved in 1 ml of distilled water and pH was set to be 7.4 via phosphate buffer saline (PBS) (Abu-Elfotuh et al., 2021). The quality of the other chemicals was of the highest grade.

### 2.2. Plant material

*Oxalis corniculata* Linn. Entire aerial parts were collected in January 2022 from the garden of Shooting Club, Dokki, Giza. The plant was taxonomically approved by the plant list website ([www.theplantlist.org](http://www.theplantlist.org)) and was authenticated by Dr. Trease Labeb, senior specialist of plant taxonomy, Orman Garden, Giza, Egypt. A voucher specimen (OC-2022) was kept at Pharmacognosy and Medicinal Plants Department, Faculty of Pharmacy (Girls), Al-Azhar University.

### 2.3. Plant extraction and sample preparation

The plant aerial parts were air-dried in the shade and then crushed. At room temperature, five hundred grams of dried powdered aerial parts were profoundly extracted by using methanol. Under vacuum by a rotary evaporator at 45 °C, methanol was totally evaporated to provide a yield of 70 g m. For ultraperformance liquid chromatography-electrospray ionization-quadrupole time-of-flight mass spectrometry (UPLC-ESI-QTOF-MS/MS) analysis, the methanolic extract of *Oxalis corniculata* (*O. corniculata* ME) was prepared by solubilizing 50 mg of this dried powdered material in 1 ml of water, methanol, and acetonitrile (2:1:1) using vortexing for 2 min and ultrasonication for 10 min. The solution was centrifuged for 10 min at 10,000 rpm 50  $\mu\text{l}$  of stock solution was diluted to 1000  $\mu\text{l}$  by reconstitution solvent. Finally, the injected concentration was 2.5  $\mu\text{g}/\mu\text{l}$ .

### 2.4. Phytochemical screening

Qualitative chemical tests were performed to identify various phytochemical categories in the entire aerial parts of *O. corniculata* (Soni and Sosa, 2013).

### 2.5. UPLC-ESI-QTOF-MS/MS analysis of *O. corniculata* ME

Exion LC system (USA) connected to an autosampler system supplied with an in-line filter disks pre-column (0.5  $\mu\text{m} \times 3$  mm, Phenomenex, USA) and an X select HSS T3 C18 column (2.5  $\mu\text{m} \times 2.1$  mm  $\times$  150 mm, Waters Corporation, Milford, MA, USA) was used under the following conditions: 40 °C, an injection volume 10  $\mu\text{l}$ , gradient elution utilizing the mobile phase, 5 mM ammonium formate containing 1% methanol (pH = 8), and a flow rate of 300  $\mu\text{L}/\text{min}$ . The MS/MS analysis was performed using a Triple TOF™ 5600+ system outfitted with a Duo Spray™ source operating in the ESI mode (AB SCIEX, Concord, Canada). The top fifteen intense ions from each scan were chosen to get the MS/MS fragmentation spectra. The target analytes were identified by correlating the UPLC/MS/MS data with the reference database (ReSpect negative, 1573 records) and the previously reported compounds (Mohammed et al., 2021, Hegazy et al., 2021).

### 2.6. Animals and experimental design

Forty male Sprague-Dawley rats (300–320 g) were procured from Nile Co., Cairo, Egypt and acclimatized for 1-week prior beginning of the work. Under normal housing conditions (25 $\pm$ 1 °C temperature and humidity (50  $\pm$  5%) with 12-h dark and light periods) in stainless steel

cages, the rats were housed at the animal house facility, Faculty of Pharmacy (Girls), Al-Azhar University. Animals were fed rodent dietary pellets and water was allowed ad libitum. Animal care and use committee of the Faculty of Pharmacy, Al-Azhar University, had approved and supervised all experimental procedures [ethical approval number (371/2023)]. All procedures and experiments were performed according to ARRIVE criteria and the relevant guidelines of the Guide for Care and Use Laboratory Animals, published by the National Institutes of Health (NIH Publications No. 8023, revised 1978).

Animals were divided in a random manner into four equal groups (n = 10) each subjected to treatment over five weeks. Group (1) served as the normal control group and was injected with normal saline (1 ml/kg). Group (2) animals were given  $\text{AlCl}_3$  (70 mg/kg i. p, daily) (Ali et al., 2016) and served as the model for Alzheimer's disease. Group (3) animals were given  $\text{AlCl}_3$  (70 mg/kg i. p, daily) + Se (1 mg/kg, p. o, daily). Group (4) animals were given  $\text{AlCl}_3$  (70 mg/kg i. p, daily) + *O. corniculata* ME (150 mg/kg, p. o, daily) (Kabach et al., 2023). The animals' behavioral tests were recorded 24 h after the last dose was administered. Animals were then sacrificed by cervical translocation, 24 h after the behavioral tests were performed, under anesthesia with ketamine (80 mg/kg, i. p.). The brains were detached, splashed with PBS (pH 7.4) and used for histological examination, as well as tissue sampling for performing biochemical analyses.

### 2.7. Evaluation of Behavioral Parameters

#### 2.7.1. Y-maze spontaneous alternation (SAP) test

SAP can reveal cognitive deficits in a sort of short-term memory called spatial working memory (Kumar et al., 2018). According to previous study (Sarter et al., 1988), a wooden, black-colored Y-shaped maze possessing a triangular symmetric center and three arms labeled A, B, or C was utilized. At the edge of one arm, animals were positioned and left for 8 min to move along the maze. The number of entries was calculated when the animal's hind paws were entered completely to the inside of the arm. SAP was measured depending on the count of alternations and total arm entries by using this formula:

$$\text{SAP (\%)} = [\text{number of alternations} / (\text{total arm entries} - 2)] \times 100.$$

#### 2.7.2. Morris water maze (MWM) test

MWM is used for evaluation of memory retention and acquisition (Morris, 1984). MWM is a water tank in a circular form (60 cm in height and 150 cm in diameter) that was filled to its half with normal water. White paint is added to water to enhance its opacity. The pool was separated into equal four quadrants (north, south, east, and west). The 10 cm diameter escape platform was hidden 2 cm beneath the surface of the water at a fixed place at the center of one of the quadrants. For 60 s, the rats were left to discover the hidden platform and then allowed to rest on it for 20 s prior to the start of the subsequent trial. If rats spent more than 60 s prior to finding the platform, they were given a rest for 20 s by gently placing them on it. The time taken by the animals to find the platform (escape latency) was noted. Clear water was used instead of the opaque one, on the fourth day and a probe test was done through letting the animals swim for 60 s, while removing the platform. The time taken in the target quadrant was recorded.

### 2.8. Preparation of tissue samples

Immediately after rats being sacrificed, brain tissues were detached and splashed by ice-cold saline. Four brains per group were kept in 10% neutral buffered formalin to be used for histopathological examination. The rest of the six brains in each group were quickly divided into two equal portions, the first one was homogenized in ice-cold Tris-HCl 50 mM (10% w/v) and 300 mM sucrose (pH 7.4) to be centrifuged at 1800 g

for 10 min at 4 °C to produce 10% homogenate (w/v), then the supernatant was used for biochemical measurements. Whereas the second portion was kept at –80 °C to be used in real time PCR analyses.

## 2.9. Biochemical analyses

### 2.9.1. Colorimetric analysis

Using colorimetric kits obtained from Biodiagnostic, Cairo, Egypt, total antioxidant capacity (TAC), superoxide dismutase (SOD), and malondialdehyde (MDA) were assessed at 510 nm, 560 nm and 534 nm wavelengths, respectively in brain tissue homogenates.

### 2.9.2. Fluorometric assays

The levels of brain monoamines (dopamine (DA), norepinephrine (NE), and serotonin (5-HT)) were evaluated by using fluorometric analysis with kits from Sigma-Aldrich Co. (St Louis, MO, USA). The fluorometric assay was done as previously described (Hamdan et al., 2022). Monoamines were detected after oxidation into their “adrenochromes,” then further reorganized to their “adrenolutins” that were identified fluorometrically at  $\lambda_{ex}/\lambda_{em}$  320/480 nm, 380/480 nm, and 355/470 nm for DA, NE, and 5-HT, for excitation and emission, respectively.

### 2.9.3. Enzyme-linked immunosorbent assay (ELISA)

ELISA technique was performed for estimating the concentration of tumor necrosis factor-  $\alpha$  (TNF- $\alpha$ ) and interleukin-1 $\beta$  (IL-1 $\beta$ ) using the Quantikine® Rat TNF- $\alpha$  ELISA Kit (catalog No: RTA00, R&D Systems, MN USA) and Cusabio Life Science, Inc., China (catalog No: CSB-E08055r), respectively. Moreover, ELISA kits from MyBioSource, Inc., San Diego, CA, USA were utilized to assess the concentration of amyloid precursor protein (APP), A $\beta$ , brain-derived neuroprotective factor (BDNF), phosphorylated tau (pTau), acetylcholinesterase (AChE),  $\beta$ -catenin, apolipoprotein E4 (ApoE4), Beclin 1,  $\beta$ -secretase enzyme (BACE1), C/EBP homologous protein (CHOP), protein kinase RNA-like endoplasmic reticulum kinase (PERK), glucose-regulated protein 78 (GRP78) and low density lipoprotein receptor-related protein 1 (LRP1) in brain tissues according to the instructions of the manufacturer.

### 2.9.4. Real-time quantitative polymerase chain reaction (RT-qPCR)

Real-time quantitative polymerase chain reaction (RT-qPCR) was used in order to assess the mRNA expression levels of nuclear factor kappa-B (*NF- $\kappa$ B*), B-cell lymphoma 2 protein (*Bcl-2*), B-cell lymphoma protein 2 (*Bcl-2*)-associated X protein (*Bax*), *caspase-1*, nucleotide-binding domain, leucine-rich-containing family, pyrin domain-containing-3 (*NLRP3*), glycogen synthase kinase-3 $\beta$  (*GSK3 $\beta$* ), *Wnt3a*, heme-oxygenase-1 (*HO-1*), nuclear factor erythroid 2-related factor 2 (*Nrf2*), toll-like receptor- 4 (*TLR4*), and the housekeeping gene ( *$\beta$ -actin*) in brain via Applied Biosystems step one plus instruments. By Qiagen tissue extraction kit (Qiagen, USA), isolation of the total RNA was done. By means of a sense rapid cDNA synthesis kit (CAT No. BIO-65053), the collected mRNA was reverse transcribed. The relative expression of target genes was got by using the following formula:  $2^{-\Delta\Delta CT}$  (Livak and Schmittgen, 2001). The sequence of primer sets is displayed in Table 1.

## 2.10. Histopathological evaluation

Brain of rats were removed and kept in 10% formalin then fixed in paraffin blocks and sectioned at 4- $\mu$ m thickness. Hematoxylin and eosin (H & E) were used to stain the slides, which were then examined by a light microscope and photomicrographs were taken at magnification of 40 $\times$  (Bancroft and Gamble, 2008).

## 2.11. Statistical analysis

The data were represented as the mean  $\pm$  SE. The statistical

**Table 1**

The sequence of primers.

Gene	Primer pair sequence	Accession number
<i>NF-<math>\kappa</math>B</i>	F:5-GGACAGCACCTACGATG-3 R:5-CTGGATCACTTCAATGGCCTC-3	NM_001276711.1
<i>Bax</i>	F: 5'-CACGTCTGCGGGGAGTCA-3' R: 5'-TAGGAAAGGAGGCCATCCCA-3'	NM_017059
<i>Bcl-2</i>	F: 5'-CATCTCATGCCAAGGGGAA-3' R: 5'-TATCCCACTCGTAGCCCTC- 3'	NM_016993
<i>Caspase -1</i>	F: 5'-GAACAAAGAAGTGGCGCAT-3' R: 5'-GAGGTCAACATCAGCTCCGA-3'	NM_012762
<i>NLRP3</i>	F: 5'-TGCATGCCGTATCTGGTTGT-3' R: 5'-ACCTCTTGCGAGGGTCTTTG-3'	NM_001191642
<i>GSK3<math>\beta</math></i>	F: 5'-AGCCTATATCCATTCCTGG-3' R: 5'-CCTCGGACCAGCTGCTT-3'	NM_032080
<i>Wnt3a</i>	F: 5'-TGCAAATGCCAGGACTATC-3' R: 5'-AGACTCTCGGTGTTTCTCTACC-3'	NM_001107005.2
<i>HO-1</i>	F:5'-CACCAGCCACAGCACTAC-3' R:5'-CACCACCCCTCAAAAGACA-3'	NM_012580
<i>Nrf-2</i>	F:5'-CTCTCTGGAGACGGCCATGACT-3' R:5'-CTGGGCTGGGACAGTGGTAGT-3'	NM_031789
<i>TLR4</i>	F: 5'-TCAGCTTTGGTCAGTTGGCT-3' R:5'-GTCCTTGACCACCTGCAAGA-3'	NM_019178
<i><math>\beta</math>-actin</i>	F: 5'-CCGTAAGACCTCTATGCCA- 3' R: 5'-AAGAAAGGGTGTAAAACGCA- 3'	NM_031144

significance between the means of different groups were analyzed statistically by one-way analysis of variance (ANOVA) followed by Tukey's post hoc test for multiple comparisons. While two-way ANOVA was used to assess the statistical analysis of the escape latency time for four days in the MWM test. Graph Pad Prism (San Diego, CA, USA) software was used to conduct statistical analyses and generate graphs (version 8.0.2). The standard for least statistical significance was at  $P < 0.05$ .

## 3. Results

### 3.1. Phytochemical screening

*Oxalis corniculata* (*O. corniculata*) entire aerial parts were subjected to a phytochemical screening, which revealed the existence of several phytoconstituents including carbohydrates, glycosides, saponins, tannins, and terpenoids, as well as trace amounts of alkaloids and no anthraquinones were detected.

### 3.2. UPLC-ESI-QTOF-MS/MS analysis of *O. corniculata* ME

Ultraperformance liquid chromatography-electrospray ionization-quadrupole time-of-flight mass spectrometry (UPLC-ESI-QTOF-MS/MS) is a sophisticated and sensitive technology that is used to detect secondary plant metabolites in complicated mixtures with high accuracy, selectivity, and sensitivity. In this work, numerous phytoconstituents were tentatively identified in the methanolic extract of *Oxalis corniculata* (*O. corniculata* ME) using a negative ESI technique. Metabolites were characterized based on their mass spectra and by comparing them to the in-house database and reference literature. Previous studies on *O. corniculata* showed the presence of flavonoids, phenolics, and cinnamic acid derivatives besides essential oils. The high-resolution, mass used in this study resulted in the tentative identification of sixty-six compounds, comprising organic acids, phenolics and others (fourteen), cinnamic acids and its derivatives (eight), fatty acids, terpenoids (seventeen) and flavonoids (twenty-seven), (Table 2, Fig. 1).

#### 3.2.1. Cinnamic acid and its derivatives

Cinnamic acid and its derivatives (eight) were identified. Rosmarinic and chlorogenic acids displayed a molecular ion peak [M-H]<sup>-</sup> at  $m/z$  at 359 and 353 respectively with appearance of a common daughter ion at  $m/z$  179 consistent with caffeic acid, while coumaroyl quinic acid displayed a molecular ion peak [M-H]<sup>-</sup> at  $m/z$  at 337 and daughter ions at

**Table 2**  
UPLC-ESI-QTOF-MS/MS analysis of *O. corniculata* ME (supplementary: Appendix 1).

Peak No.	[M-H] <sup>-</sup>	Precursor (m/z)	Δ ppm	Tentatively identified compounds	RT (min.)	Identified fragments (MS <sup>2</sup> ions)
<b>Organic acids, phenolics and others (14)</b>						
1	C <sub>4</sub> H <sub>6</sub> O <sub>5</sub>	133.0137	4.1	Malic acid	0.96	133, 115, 73
2	C <sub>9</sub> H <sub>7</sub> O <sub>9</sub>	259.0087	0.9	Cinnamaldehyde	1.06	259, 153, 133, 78
3	C <sub>6</sub> H <sub>12</sub> O <sub>6</sub>	179.0563	3.8	Glucose	1.11	179, 161, 75, 73
4	C <sub>6</sub> H <sub>12</sub> O <sub>7</sub>	195.0515	2.9	Gluconic acid	1.13	195, 129, 75
5	C <sub>14</sub> H <sub>18</sub> O <sub>9</sub>	329.0901	-4.3	Vanillic acid hexoside	1.19	329, 271, 167 (-162), 93
6	C <sub>12</sub> H <sub>22</sub> O <sub>11</sub>	341.1091	3.7	Sucrose	1.3	161, 179, 89
7	C <sub>13</sub> H <sub>16</sub> O <sub>8</sub>	299.0767	1.9	Salicylic acid hexoside	1.39	299, 253, 193, 137, 93
8	C <sub>6</sub> H <sub>9</sub> O <sub>8</sub>	209.0301	4.3	Mucic acid	1.45	164, 125, 59
9	C <sub>13</sub> H <sub>15</sub> O <sub>9</sub>	315.1068	-2	Vanillyl beta-D-glucopyranoside	2.33	315, 153, 109
10	C <sub>7</sub> H <sub>8</sub> O <sub>3</sub>	137.02442	2	Hydroxybenzoate	3.26	137, 93, 65
11	C <sub>7</sub> H <sub>6</sub> O <sub>4</sub>	153.0183	0.4	Dihydroxybenzoate (Protocatechuic acid)	4.15	153, 113, 85
12	C <sub>19</sub> H <sub>28</sub> O <sub>10</sub>	415.1596	-0.7	Benzyl alcohol -O-hexosyl rhamnoside	4.54	415, 278, 210, 102
13	C <sub>18</sub> H <sub>25</sub> O <sub>10</sub>	401.1429	-6	Benzyl alcohol-O-pentosyl-hexoside	4.87	401, 294, 188
14	C <sub>19</sub> H <sub>30</sub> O <sub>8</sub>	385.1875	4.7	Hydroxy jasmonic acid hexoside	18.1	385, 223,153
<b>Cinnamic acid and its derivatives (8)</b>						
15	C <sub>18</sub> H <sub>18</sub> O <sub>9</sub>	377.0857	-2.7	Caffeic acid derivative	1.26	341, 215, 179
16	C <sub>16</sub> H <sub>18</sub> O <sub>9</sub>	353.08797	3.7	Chlorogenic acid	1.49	353, 294, 191, 179, 161, 85
17	C <sub>9</sub> H <sub>8</sub> O <sub>2</sub>	147.04406	2.3	Cinnamic acid	1.9	147, 103
18	C <sub>16</sub> H <sub>18</sub> O <sub>8</sub>	337.09512	1.8	Coumaroyl quinic acid	2.87	337, 191, 163, 143, 114
19	C <sub>15</sub> H <sub>20</sub> O <sub>8</sub>	327.1079	1.4	Coumaric acid hexoside	3.79	258, 191, 147, 113
20	C <sub>28</sub> H <sub>26</sub> O <sub>14</sub>	585.12620	4.88	1,3-Dicaffeoyl-5-malonyl-δ-quinide	4	585, 522, 465, 375, 294, 256, 189
21	C <sub>18</sub> H <sub>16</sub> O <sub>8</sub>	359.07717	-0.2	Rosmarinic acid	4.46	359, 313, 193, 179, 161, 123
22	C <sub>29</sub> H <sub>28</sub> O <sub>16</sub>	631.1304	1.6	1-O,5-O-Dicaffeoyl-3-O-(2-hydroxysuccinyl) quinic acid	5.04	631, 563, 353
<b>Flavonoids (27)</b>						
23	C <sub>27</sub> H <sub>30</sub> O <sub>15</sub>	593.1511	1.7	Isovitexin hexoside	4.14	593,473,383,353
24	C <sub>21</sub> H <sub>24</sub> O <sub>10</sub>	435.128	4.7	Phloretin hexoside (dihydrochalcone)	4.58	435, 345, 315 (-120), 297, 190, 151
25	C <sub>27</sub> H <sub>29</sub> O <sub>16</sub>	563.14130	3.1	Apigenin-O-pentosyl-hexoside	4.9	563, 443, 353
26	C <sub>21</sub> H <sub>18</sub> O <sub>12</sub>	461.0718	0.8	Luteolin glucuronide	4.91	461, 285
27	C <sub>27</sub> H <sub>34</sub> O <sub>14</sub>	581.1846	-3.2	Naringin dihydrochalcone	5.19	581, 491, 461, 299, 269, 193
28	C <sub>21</sub> H <sub>18</sub> O <sub>11</sub>	445.0766	2.7	Apigenin glucuronide	5.52	445, 269, 175, 113
29	C <sub>22</sub> H <sub>20</sub> O <sub>12</sub>	475.0915	3.4	Chrysoeriol-7-O-glucuronide	5.82	475, 299, 284, 257, 188, 175, 113, 59
30	C <sub>23</sub> H <sub>23</sub> O <sub>12</sub>	491.1188	3.9	Tricin hexoside (dihydroxydimethoxy flavone hexoside)	6.03	491, 422, 354, 218, 152
31	C <sub>21</sub> H <sub>19</sub> O <sub>12</sub>	463.0896	5.4	Quercetin hexoside	6.11	463, 400, 300, 254,188
32	C <sub>21</sub> H <sub>22</sub> O <sub>9</sub>	417.1198	4.3	Isoliquiritin	6.16	417, 310, 294, 255
33	C <sub>27</sub> H <sub>30</sub> O <sub>15</sub>	593.1528	4.6	Luteolin hexosylrhamnoside	6.44	593, 400, 285
34	C <sub>27</sub> H <sub>30</sub> O <sub>14</sub>	577.1754	0.4	Vitexin rhamnoside	7.43	577, 508, 400, 269
35	C <sub>28</sub> H <sub>31</sub> O <sub>15</sub>	607.1681	3.9	Diosmin	7.52	607, 299, 284
36	C <sub>21</sub> H <sub>20</sub> O <sub>10</sub>	431.0972	1.2	Apigenin hexoside	7.55	431, 269
37	C <sub>22</sub> H <sub>23</sub> O <sub>11</sub>	461.1091	2.7	Trihydroxy-7-methoxy-3-(α-L-rhamnopyranosyloxy) flavone	7.7	461, 446, 400, 256, 175
38	C <sub>15</sub> H <sub>10</sub> O <sub>4</sub>	253.0499	-2.9	Chrysin	8.25	253, 135, 117
39	C <sub>16</sub> H <sub>12</sub> O <sub>5</sub>	283.0612	3.9	Acacetin (Dihydroxy methoxyflavone)	8.52	283, 268, 135
40	C <sub>16</sub> H <sub>13</sub> O <sub>6</sub>	301.0696	-3.5	Hesperitin	8.10	301, 283, 269, 255, 224, 177, 167
41	C <sub>22</sub> H <sub>19</sub> O <sub>11</sub>	459.0928	1.3	Apigenin 7-O-methylglucuronide	9.17	269
42	C <sub>16</sub> H <sub>13</sub> O <sub>5</sub>	285.0757	-0.2	Dihydroxymethoxyflavanone (methyl naringenin)	9.51	285, 149,133
43	C <sub>15</sub> H <sub>10</sub> O <sub>5</sub>	269.0454	3.3	Apigenin	10.06	269, 225, 151, 149, 117
44	C <sub>30</sub> H <sub>20</sub> O <sub>10</sub>	539.0982	1.7	Rhusflavone (biapigenin)	10.13	269
45	C <sub>16</sub> H <sub>11</sub> O <sub>6</sub>	299.0562	4	Chrysoeriol (trihydroxymethoxyflavone)	10.39	299, 285, 256
46	C <sub>15</sub> H <sub>9</sub> O <sub>6</sub>	285.03936	2.9	Luteolin	10.50	285, 269, 133
47	C <sub>15</sub> H <sub>12</sub> O <sub>4</sub>	255.0666	5.5	Isoliquiritigenin (3.4e4)	11.38	255, 135, 119
48	C <sub>16</sub> H <sub>12</sub> O <sub>4</sub>	267.0659	2.7	Tectochrysin (methoxyhydroxy flavone)	11.85	267, 252 (-15), 223, 132
49	C <sub>17</sub> H <sub>16</sub> O <sub>5</sub>	299.0914	0	Hydroxy deimethoxy flavanone (4',7-Di-O-methylnaringenin)	12.57	299, 283, 269
<b>Fatty acids, terpenoids and hydrocarbons (17)</b>						
50	C <sub>9</sub> H <sub>18</sub> O <sub>10</sub>	285.0818	0.6	2,3,4,4,5,6,7,8,9-Nonahydroxynonanal	1.27	285, 131, 113, 70
51	C <sub>18</sub> H <sub>30</sub> O <sub>3</sub>	293.21170	2	17-Hydroxylinolenic acid	12.74	293, 221, 181
52	C <sub>16</sub> H <sub>32</sub> O <sub>3</sub>	271.2281	4.9	2-Hydroxypalmitic acid	14.31	271, 225
53	C <sub>18</sub> H <sub>30</sub> O <sub>2</sub>	277.21780	4.7	Linolenic acid	17.12	277, 208, 102
54	C <sub>18</sub> H <sub>34</sub> O <sub>6</sub>	345.2273	0.4	9,10-Dihydroxyoctadecanedioic acid)	17.77	345, 277, 208
55	C <sub>21</sub> H <sub>35</sub> O <sub>4</sub>	351.2514	-4.5	Linolenoyl glycerol	26.65	351, 283
56	C <sub>18</sub> H <sub>34</sub> O <sub>4</sub>	313.23740	0.2	Octadecanedioic acid	15.84	313, 294, 188, 75
57	C <sub>18</sub> H <sub>32</sub> O <sub>2</sub>	279.2330	4.1	Linoleic acid	19.48	279, 211, 103
58	C <sub>22</sub> H <sub>42</sub> O <sub>2</sub>	337.31057	1.5	Erucic acid	19.49	337, 269, 245, 185
59	C <sub>20</sub> H <sub>32</sub> O <sub>2</sub>	303.2339	-3.5	Arachidonic acid	20.02	303, 191, 113, 99
60	C <sub>15</sub> H <sub>30</sub> O <sub>2</sub>	241.2172	4.1	Pentadecanoic acid	19.82	241, 155, 105
61	C <sub>18</sub> H <sub>36</sub> O <sub>2</sub>	283.2634	0.9	Stearic acid	20.69	283, 268, 224, 135, 91
62	C <sub>9</sub> H <sub>17</sub> O <sub>2</sub>	157.1216	-4.5	Nonanoic acid	20.64	157, 126, 99, 91,60
63	C <sub>17</sub> H <sub>32</sub> O <sub>2</sub>	267.2330	0.3	Methyl palmitoleate	20.85	267, 113
64	C <sub>16</sub> H <sub>31</sub> O <sub>2</sub>	255.2333	1.4	Palmitic acid	21.41	255,146
65	C <sub>20</sub> H <sub>34</sub> O <sub>2</sub>	305.2488	4.2	Ethyl linolenate	21.77	305, 113
66	C <sub>30</sub> H <sub>48</sub> O <sub>3</sub>	455.3524	-0.4	Oleanolic acid	22.44	455

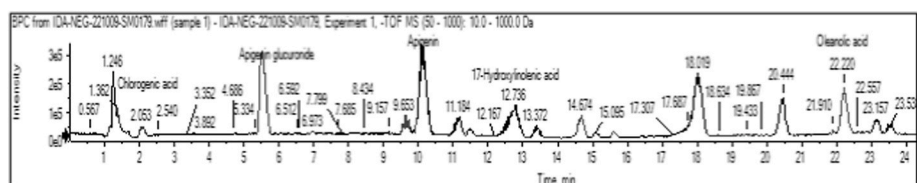


Fig. 1. UPLC/MS base peak chromatogram of *Oxalis corniculata* ME. Detections in negative ionization mode showing major secondary metabolites.

$m/z$  191 and 143 besides other di-caffeoyl quinic acid derivatives. (Sik et al., 2019; Bakr et al., 2016).

### 3.2.2. Flavonoids

*O. corniculata* ME exhibited different classes of flavonoid. Flavones and flavonols constitute the vast majority of the flavan-based flavonoids. Flavones appeared as the predominant class, represented by apigenin with  $[M-H]^-$  at  $m/z$  269 and daughter ion peaks at 225, 151, 117, whereas peak at 117 is diagnostic of ring C cleavage at 1/3 (Liu et al., 2010). Additionally, apigenin glucuronide was noted at  $[M-H]^-$  445 and major fragments at  $m/z$  269 and 175. Apigenin methyl glucuronide was also identified at  $m/z$  459. Glycosides also appeared where apigenin hexoside  $[M-H]^-$  at  $m/z$  431, isovitexin hexoside  $[M-H]^-$  at  $m/z$  593 with characteristic fragment ions at  $m/z$  473  $[M-H-120]^-$ , 383  $[M-H-120-90]^-$ , and 353 consistent with C-glycosidic bonds, and vitexin rhamnoside  $[M-H]^-$  at  $m/z$  577 (Zhang et al., 2010). Luteolin and its glycosides have also been recognized, where the aglycone showed up at  $[M-H]^-$  at  $m/z$

285, which appeared as a major fragment in the identified glycoside including luteolin glucuronide  $[M-H]^-$  at  $m/z$  461 and luteolin hexosyl rhamnoside at  $m/z$  593. Many methoxylated flavones have been detected among them acacetin (methoxy apigenin) which has been tentatively identified with  $[M-H]^-$  at  $m/z$  283 and daughter ion peaks at  $m/z$  269  $[M-H-15]^-$  and 135 and chrysoeriol (methoxylated luteolin) distinguished at  $m/z$  299 in addition to its glucuronide with  $[M-H]^-$  at  $m/z$  475.

Flavanone has also been identified, where naringenin, isoliquiritin and isoliquiritigenin and hesperitin have been identified. From the common fragments in the flavanone chromatogram is  $[M-H-H_2O]^-$  produced by dehydration of the flavanone molecule, where hesperitin at  $m/z$  301 showed a daughter ion peaks at  $m/z$  283  $[M-H-H_2O]^-$ . Chalcones observed included phloretin hexoside with  $[M-H]^-$  at  $m/z$  at 435 and daughter ions at  $m/z$  345  $[M-H-90]^-$  and 315  $[M-H-120]^-$ , and naringin dihydrochalcone at  $[M-H]^-$  at  $m/z$  581 (Zhang et al., 2008).

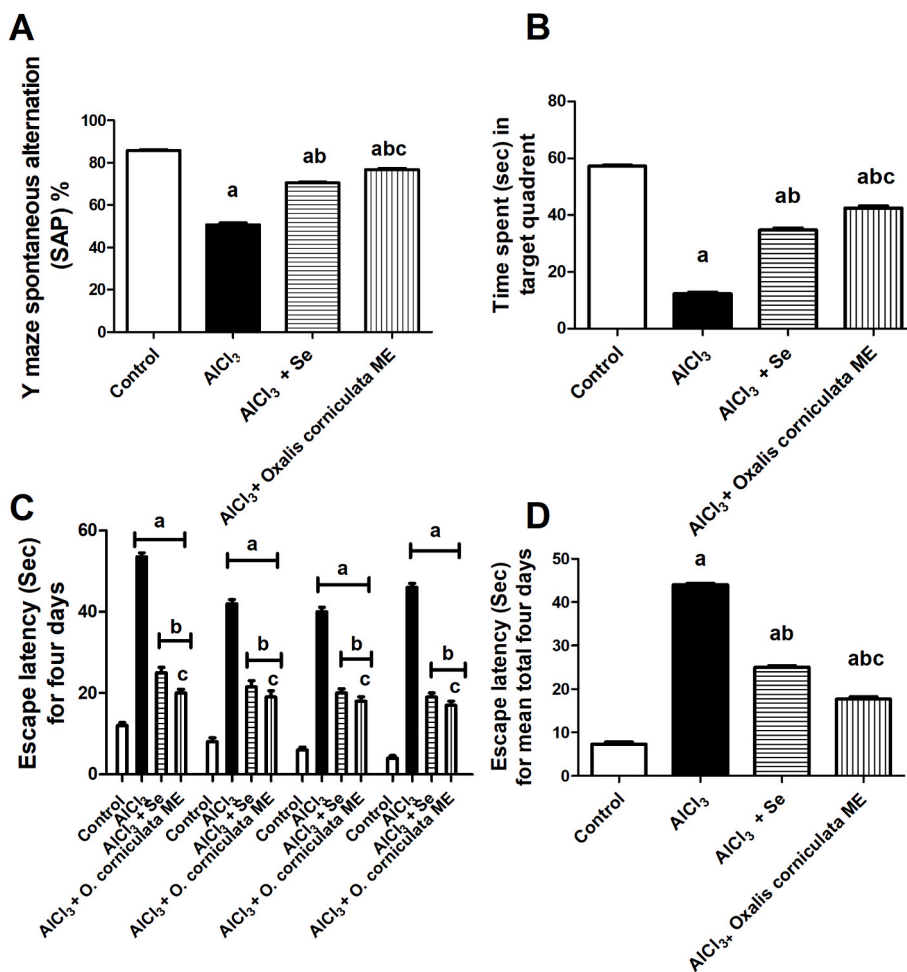


Fig. 2. Effect of *O. corniculata* ME and Se on Behavioral Parameters in  $AlCl_3$ -induced AD in Rats. (A) SAP (%) in Y- Maze test, (B) Time spent (Sec) in target quadrant, (C) Escape latency (Sec) for four days in the MWM test, (D) Escape latency (Sec) for mean total four days in the MWM test. <sup>a</sup> Significantly different from control group at  $p < 0.05$ . <sup>b</sup> Significantly different from  $AlCl_3$  group at  $p < 0.05$ . <sup>c</sup> Significantly different from  $AlCl_3 + Se$  group at  $p < 0.05$ .

### 3.2.3. Fatty acids, terpenoids and hydrocarbons

Fatty acids varying between unsaturated and saturated have been identified showing typical loss of H<sub>2</sub>O [M - H-18]<sup>-</sup> and/or loss of carboxylic moieties [M - H- 44]<sup>-</sup> (Han, 2016) including linoleic, linolenic, arachidonic, and palmitic acids as well as their derivatives. Triterpenoid compound (oleanolic acid) has also been identified (Table 2).

### 3.3. The effect of the methanolic extract of *Oxalis corniculata* linn (*O. corniculata* ME) and selenium (Se) on Behavioral Parameters in AlCl<sub>3</sub>-induced AD in rats

#### 3.3.1. Y-maze spontaneous alternation test

In Y-Maze spontaneous alternation, there was noticeable drop in SAP % in AlCl<sub>3</sub>-intoxicated rats in comparison to the control group (42.53%). Nevertheless, this lessening was significantly improved by Se and *O. corniculata* ME administration compared with the AD rats. However, *O. corniculata* ME showed a significant improvement in cognitive deficits in spatial working memory of AD rats (returned to the normal SAP% of control group) compared to Se therapy, (Fig. 2A).

#### 3.3.2. Morris water maze test (MWM)

The MWM test results showed that the AlCl<sub>3</sub>-intoxicated rats elicited a marked reduction and deterioration in their spatial learning as evidenced by the significantly higher mean escape latency (5.7 time) to find the platform (Fig. 2C and D) and the decrease in the time expended in the target quadrant (83.59%), over the span of four days, in comparison to control group (Fig. 2 B). The learning and spatial memory deficits resulted from AlCl<sub>3</sub> were improved by Se and *O. corniculata* ME administration, as demonstrated by the reduction of the mean escape latency over the four days (50.78 and 64.91% respectively) and the increment in the time spent in the target quadrant (3.1 and 4.23 times respectively) compared to AlCl<sub>3</sub> control group. It is noteworthy that *O. corniculata* ME treated group showed the best results in the escape latency and the maximum time spent in the target quadrant in comparison to Se treated group.

#### 3.4. The effect of *O. corniculata* ME and Se on antioxidant parameters; TAC and SOD, Gene Expression of Oxidative Stress Markers Nrf2 and HO-1 and neurotransmitters levels (DA, 5-HT, NE, and ACHE) in brain tissue of AlCl<sub>3</sub>-induced AD in rats

AlCl<sub>3</sub> administration displayed a remarkable increase in oxidative stress indicated by a remarkable decrease in endogenous antioxidants represented as TAC by 75 % and a significant reduction of SOD levels by 86 % and rising MDA level by 18 folds in brain tissues when compared to control. Moreover, brain monoamines (DA, 5-HT, and NE) were reduced by 81%, 61%, 65% respectively, while ACHE level was increased by 231 % in AlCl<sub>3</sub>-intoxicated group relative to the control group. Conversely, Se administration along with AlCl<sub>3</sub> exposure fixed the brain's TAC and SOD levels and exerted a marked reduction in brain MDA level when compared to AlCl<sub>3</sub> control group. Moreover, Se therapy improved the levels of neurotransmitters and prevented the heightened levels of ACHE caused by AlCl<sub>3</sub> relative to AlCl<sub>3</sub>-control group. Similarly, *O. corniculata* ME significantly improved the level of endogenous antioxidants observed through the rise of TAC as well as SOD activity coupled with a marked decrease in MDA level in brain tissue when compared to the group receiving AlCl<sub>3</sub>. The levels of DA, 5-HT, NE, and ACHE were significantly ameliorated when compared to AlCl<sub>3</sub>-intoxicated group, (Table 3).

Nrf2 and HO-1 gene expressions were pronouncedly decreased in rats treated with AlCl<sub>3</sub> by 77% and 72%, respectively, when compared to the normal control group (Fig. 3A and B). Conversely, Se reactivated Nrf2/HO-1 signaling by upregulating mRNA expressions of Nrf2 and HO-1 by 95 % and 97 %, respectively compared to the AlCl<sub>3</sub> group thus resulting in neuroprotective effects. Similarly, *O. corniculata* ME showed neuroprotective results by exhibiting a marked rise in the mRNA

**Table 3**

The effect of *O. corniculata* ME and Se on antioxidant parameters and neurotransmitters levels in brain tissue of AlCl<sub>3</sub>-induced AD in rats.

Parameters	Groups			
	Control	AlCl <sub>3</sub>	AlCl <sub>3</sub> + Se	AlCl <sub>3</sub> + <i>O. corniculata</i> ME
TAC (umol/g tissue)	46.45 ± 0.20	11.63 ± 0.28 <sup>a</sup>	27.77 ± 0.45 <sup>ab</sup>	33.03 ± 0.69 <sup>abc</sup>
SOD (U/g tissue)	6.37 ± 0.17	0.87 ± 0.01 <sup>a</sup>	3.82 ± 0.05 <sup>ab</sup>	4.43 ± 0.06 <sup>abc</sup>
MDA (nmol/g tissue)	5.97 ± 0.22	105.20 ± 2.68 <sup>a</sup>	59.82 ± 1.22 <sup>ab</sup>	42.77 ± 1.45 <sup>abc</sup>
DA (ng/g tissue)	69.72 ± 0.47	13.47 ± 0.35 <sup>a</sup>	43.48 ± 0.37 <sup>ab</sup>	54.62 ± 0.24 <sup>abc</sup>
5-HT (ng/g tissue)	12.15 ± 0.18	4.72 ± 0.09 <sup>a</sup>	6.73 ± 0.20 <sup>ab</sup>	8.65 ± 0.16 <sup>abc</sup>
NE (nmol/g tissue)	738.90 ± 0.63	261.00 ± 3.00 <sup>a</sup>	443.20 ± 5.21 <sup>ab</sup>	537.3 ± 8.09 <sup>abc</sup>
ACHE (ng/g tissue)	10.97 ± 0.31	36.32 ± 0.38 <sup>a</sup>	19.02 ± 0.41 <sup>ab</sup>	16.18 ± 0.41 <sup>abc</sup>

Data were expressed as means ± SE (n = 6). <sup>a</sup> Significantly different from control group at p < 0.05. <sup>b</sup> Significantly different from AlCl<sub>3</sub> group at p < 0.05. <sup>c</sup> Significantly different from AlCl<sub>3</sub> + Se group at p < 0.05.

expressions of Nrf2 and HO-1 by 0.95 and 1.57 times respectively compared to the AlCl<sub>3</sub> treated group. However, *O. corniculata* ME also had a notable better effect on the antioxidant biomarkers compared to that of Se.

#### 3.5. The effect of *O. corniculata* ME and Se on Neuroinflammatory Biomarkers: NF-kB, TLR4, NLRP3, Caspase-1, TNF-α and IL-1β in the brain tissue of AlCl<sub>3</sub>-induced AD in rats

The mRNA expression of the inflammatory markers *NF-kB* and *TLR4* were upregulated 6 and 8 times, respectively, in AD rats compared to control group. In parallel, IL-1β and TNF-α contents were both significantly elevated by 5 folds. Se administration notably inhibited the inflammatory surge produced by AlCl<sub>3</sub> in rats. The mRNA expression of *TLR4* was abridged by 47% after administration of Se. Moreover, Se produced a remarkable decline in IL-1β and TNF-α contents by 52% and 48%, respectively, with concurrent reduction in *NF-kB* gene expression by 40%, when compared to AD group.

*O. corniculata* ME also resulted in a remarkable decline in the level of IL-1β amounting to 69% as well as a notable lower level of TNF-α equal to 63%. The latter was coupled with a considerable decrease in *NF-kB* and *TLR4* gene expressions by 57% and 55%, respectively. The gene expression of *NLRP3* and *caspase-1* were both markedly increased in the AlCl<sub>3</sub>-intoxicated group relative to the control group by 9 folds. Se therapy decreased the expression of *NLRP3* inflammasome, by 21%. By the same token, *caspase-1* gene expression exhibited a remarkable decrement by 55% in comparison to the AlCl<sub>3</sub>-intoxicated group. *O. corniculata* ME also alleviated the effects of AlCl<sub>3</sub> by downregulating the gene expression of *NLRP3* and *caspase-1* by 48% and 62%, respectively. Additionally, *O. corniculata* ME showed a significant effect in the restoration of the inflammasome activation biomarkers compared to the effect of Se. As presented in (Fig. 4A–F). *O. corniculata* ME showed maximum restoring activity in the inflammatory biomarkers in comparison to Se treatment.

#### 3.6. The effect of *O. corniculata* ME and Se on Apoptosis Biomarker; *bax/bcl-2*, autophagy initiating protein, *beclin 1* and the cognitive biomarker; *BDNF* in brain tissue of AlCl<sub>3</sub>-induced AD in rats

AlCl<sub>3</sub>-intoxicated rats experienced a notable increase in the expression of the *Bax* gene by about 4.42 times as compared to the control group. Compared to AD rats, the latter effect was enhanced by the administration of Se, which considerably lowered the high *Bax* level by

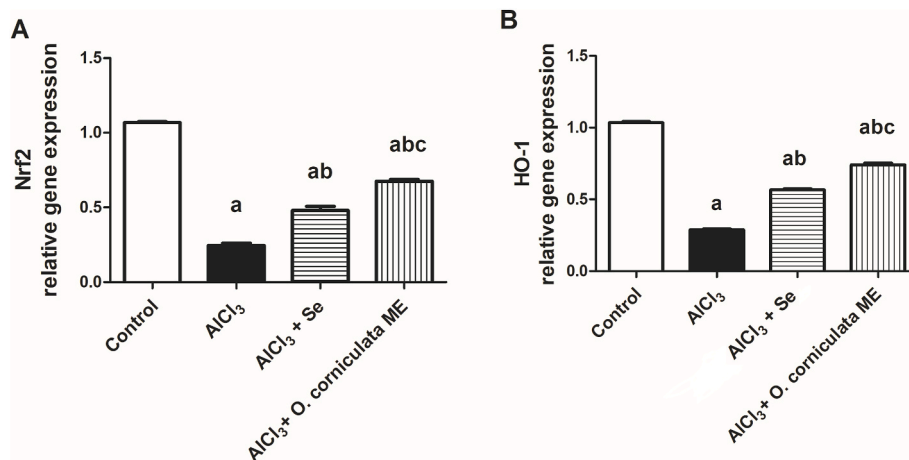


**Fig. 3.** Effect of *O. corniculata* ME and Se Modulation on the Gene Expression of Oxidative Stress Markers, *Nrf2* and *HO-1* in Brain Tissue of  $AlCl_3$ -induced AD in Rats. Relative gene expression of (A) *Nrf2* and (B) *HO-1*. <sup>a</sup> Significantly different from control group at  $p < 0.05$ . <sup>b</sup> Significantly different from  $AlCl_3$  group at  $p < 0.05$ . <sup>c</sup> Significantly different from  $AlCl_3 + Se$  group at  $p < 0.05$ .

25%. On the other hand, *O. corniculata* ME elicited a prominent decline in *Bax* mRNA expression by about 42% compared to AD rats. *Bcl-2* gene expression level was significantly lower in rats receiving  $AlCl_3$  by 84% than in control rats, but after receiving Se, *Bcl-2* gene expression levels notably increased by 368% compared to AD rats. Also, the group of rats administered *O. corniculata* ME showed a noticeable increase in *Bcl-2* gene expression by 409% compared to AD rats (Fig. 5A and B).

The level of the autophagy regulating protein, Beclin 1 was found to be markedly reduced in AD rats by 98% when compared to control. Upon administration of Se the level of Beclin1 was dramatically increased by 43 folds while the administration of *O. corniculata* ME caused a significant rise in the protein level by about 31 folds compared to AD rats (Fig. 5C).

Meanwhile, the cognitive biomarker BDNF was markedly diminished by 70% in AD group in comparison to the control group. Contrarily, Se administration considerably increased the BDNF protein level, by about 131%. In the meantime, *O. corniculata* ME showed a marked increase in BDNF level by 180% relative to AD rats (Fig. 5D). It was noted that *O. corniculata* ME had a significantly ameliorating effect on apoptosis and autophagy biomarkers when compared to AD rats receiving Se therapy. On the other hand, Se therapy showed a better effect level of the cognitive protein, BDNF.

### 3.7. Effect of *O. corniculata* ME and Se on potential AD biomarkers (BACE1, $A\beta$ Generation, APP, and p-tau levels) in brain tissue of $AlCl_3$ -induced AD in rats

AD rats exhibited a remarkable increase in BACE1 activity and APP level by about 10 and 20-folds, respectively (Fig. 6 A, B), which sequentially raised the level of  $A\beta$  by 17 folds relative to control group (Fig. 6 C). Furthermore, the level of p-Tau showed a marked increase by 31-folds. (Fig. 6 D). On the other hand, Se administration hindered  $A\beta$  generation and Tau hyperphosphorylation. BACE1 level was significantly decreased by about 40%, likewise APP,  $A\beta$  and p-Tau levels were lessened by 66%, 48% and 42%, respectively relative to AD group. In the same manner, *O. corniculata* ME treatment showed significantly lower levels of BACE1,  $A\beta$ , APP and p-Tau by 56%, 61%, 80% and 67%, respectively compared to AD rats. *O. corniculata* ME displayed a significantly superior ameliorating activity in restoring AD biomarkers compared to the effects of Se.

### 3.8. Effect of *O. corniculata* ME and Se on potential modulation of the neuronal receptor; LRP1 and pathophysiology biomarker; ApoE4 in brain tissue of $AlCl_3$ -induced AD in rats

$AlCl_3$  treatment resulted in an aggravated decrease in the level of LRP1 protein expression by 69% and a significant rise in the protein expression of ApoE4 by 17 folds when compared to control, as shown in (Fig. 7 A, B). The administration of Se therapy and *O. corniculata* ME resulted in a marked improvement in LRP1 protein expression of 1.19 and 1.97 times, respectively, when compared to rats receiving  $AlCl_3$  alone. Likewise, a significant improvement in ApoE4 protein expression was observed upon administration of Se by 62% and *O. corniculata* ME by 72%. *O. corniculata* ME achieved the maximum effects in restoring the AD pathophysiology biomarker and the modulation of the neuronal receptor LRP1 compared to the effects of Se.

### 3.9. Effect of *O. corniculata* ME and Se on wnt3a/ $\beta$ -catenin/GSK3 $\beta$ pathway in brain tissue of $AlCl_3$ -induced AD in rats

$AlCl_3$  exerted pronounced reduction of both Wnt3a and  $\beta$ -Catenin by 86 % and 94%, respectively in comparison to control group. Meanwhile, GSK3 $\beta$  expression was markedly elevated by 10 folds in  $AlCl_3$ -intoxicated rats in comparison to control group. However, these changes were changed remarkably upon the administration of Se and *O. corniculata* ME compared with the  $AlCl_3$ -intoxicated group. Se and *O. corniculata* ME demonstrated a significant improvement in restoring the Wnt3a/ $\beta$ -Catenin/GSK3 $\beta$  signaling pathway where Se administration caused a notable rise in both Wnt 3 and  $\beta$ -Catenin by 3 and 8 folds, respectively while GSK3 $\beta$  gene expression showed a significant decrease by 38% in comparison to  $AlCl_3$ -control rats. By the same token, *O. corniculata* ME administration resulted in a significant increase in Wnt3a and  $\beta$ -Catenin by around 5 and 8 folds, respectively and a notable reduction in GSK3 $\beta$  gene expression by 49 % relative to the group receiving  $AlCl_3$  (Fig. 8 A-C). *O. corniculata* ME possesses the maximum effects for restoring of the Wnt3a/ $\beta$ -catenin/GSK3 $\beta$  signaling pathway relative to that of Se.

### 3.10. The effect of *O. corniculata* ME and Se on activation of ER stress-induced Cell Death Protein; CHOP and UPR genes; PERK and GRP78 in brain tissue of $AlCl_3$ -induced AD in rats

The level of CHOP protein was dramatically elevated by 62 folds in the AD rats when compared to control rats. By the same token both PERK and GRP78 levels were significantly increased by 61 and 346 folds, respectively. While Se administration resulted in a notable decrease in

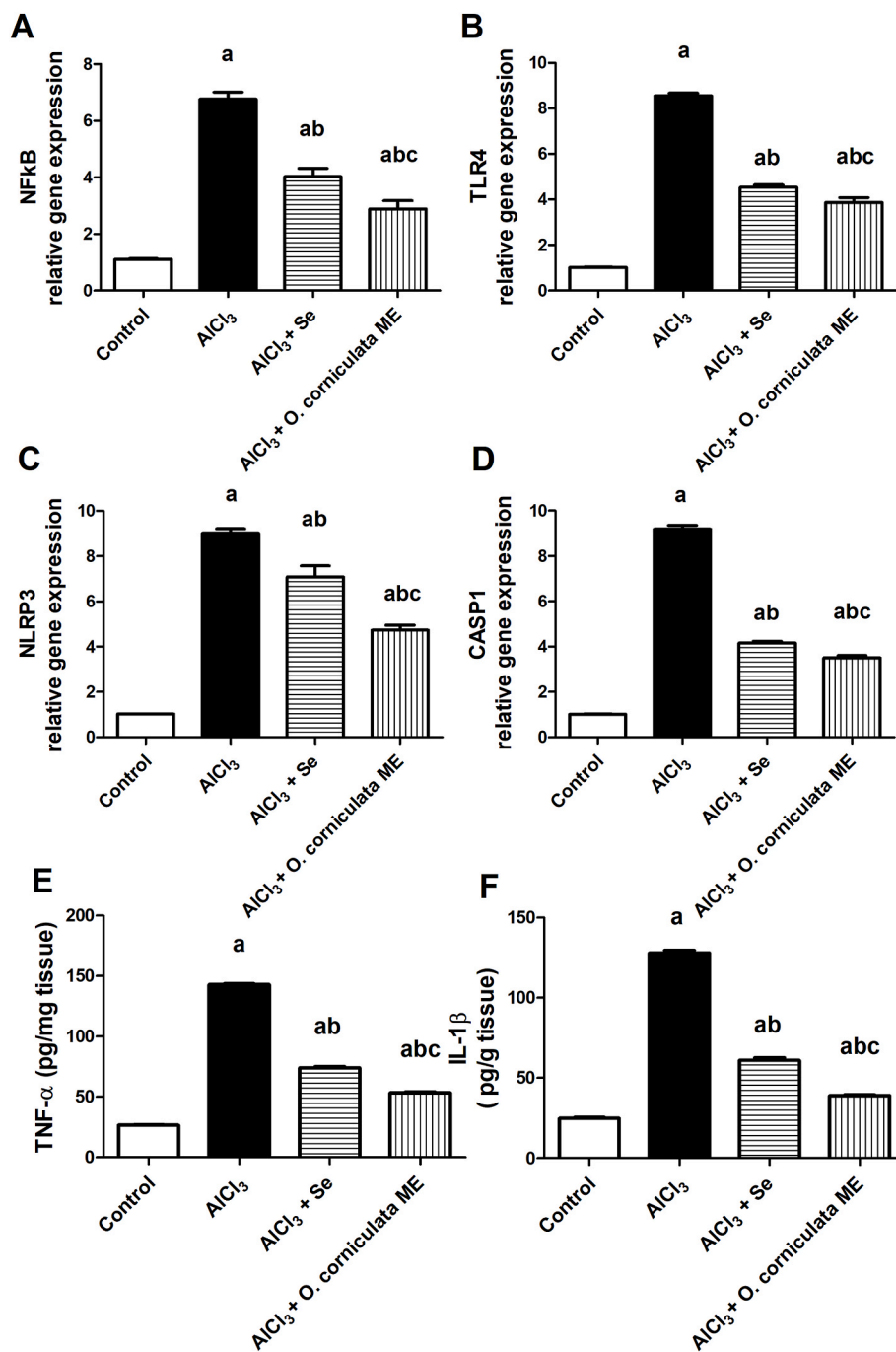


**Fig. 4.** Effect of *O. corniculata* ME and Se on Neuroinflammatory Biomarkers: *NF-kB*, *TLR4*, *NLRP3*, *Caspase-1*, *TNF-α* and *IL-1β* in the Brain Tissue of  $\text{AlCl}_3$ -induced AD in Rats. Relative gene expression of (A) *NF-kB*, (B) *TLR4*, (C) *NLRP3* and (D) *Caspase-1* along with (E) *TNF-α* level and (F) *IL-1β* level. <sup>a</sup> Significantly different from control group at  $p < 0.05$ . <sup>b</sup> Significantly different from  $\text{AlCl}_3$  group at  $p < 0.05$ . <sup>c</sup> Significantly different from  $\text{AlCl}_3$ + Se group at  $p < 0.05$ .

CHOP level by 52% also a marked decrease in PERK and GRP78 by 44 % and 25 %, respectively compared to AD rats. Similarly, *O. corniculata* ME showed a significant amelioration in levels of CHOP, PERK and GRP78 by 62%,53% and 50 %, respectively. The previous results indicated that *O. corniculata* ME exhibited a significantly improvement in ER stress induced cell death pathway compared to Se (Fig. 9 A-C).

### 3.11. Histopathological evaluation of brain tissues

The brain tissues of the untreated group displayed normal architecture without any abnormal histological changes. Whereas the  $\text{AlCl}_3$  group, most of neuronal cells of the cerebral cortex, as well as the

subiculum and fascia dentate of the hippocampus, exhibited nuclear pyknosis and degeneration. In addition, in the striatum, large size eosinophilic plaques were formed coupled with neuronal loss. Se administration exhibited nuclear pyknosis and fewer neuronal loss in the cortex and hippocampus while no histopathological changes were observed in the striatum. The histological alterations were greatly improved upon the administration of *O. corniculata* ME showing remarkable results where histoarchitectural changes were minor particularly the cortex and hippocampus except for small size focal eosinophilic plaques with neuronal loss were seen in the striatum (Fig. 10 A-P).

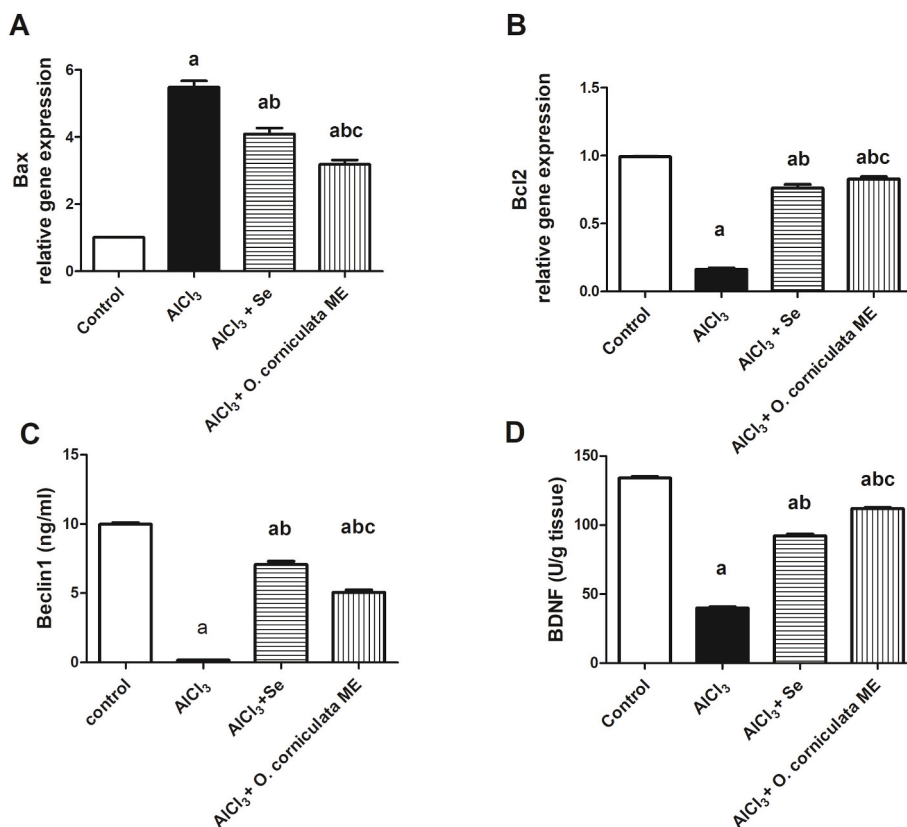


**Fig. 5.** Effect of *O. corniculata* ME and Se on Apoptosis Biomarker; Bax/Bcl-2, Autophagy Initiating Protein Beclin 1 and the Cognitive Biomarker; BDNF in Brain Tissue of AlCl<sub>3</sub>-induced AD in Rats. Relative gene expression of (A) *Bax* and (B) *Bcl-2*, together with (C) Beclin1 level and (D) BDNF level. <sup>a</sup> Significantly different from control group at  $p < 0.05$ . <sup>b</sup> Significantly different from AlCl<sub>3</sub> group at  $p < 0.05$ . <sup>c</sup> Significantly different from AlCl<sub>3</sub> + Se group.

#### 4. Discussion

The present work investigated and compared the beneficial actions of the methanolic extract of *Oxalis corniculata* (*O. corniculata* ME) and the micronutrient selenium (Se) against AlCl<sub>3</sub>-induced AD, through exploring their effect on interrelated axes, namely, Nrf2/HO-1, TLR4/NLRP3, APOE4/LRP1, Wnt 3/ $\beta$ -catenin/GSK-3 $\beta$  and PERK axes.

In this study Se has been used as a positive control to compare its neuroprotective effect to *O. corniculata* ME extract. Se has been proven to be an antioxidant, and its deficiency can compromise brain functions. Previous studies suggested that Se can enhance the neurotoxic effect of various compounds such as arsenic and lead (Khalil et al., 2022). Se also has a pivotal role in preserving neurological activity such as locomotor activity, coordination, memory, cognition, and signal transmission. The neuroprotective effects of Se are elucidated by its physicochemical properties, its capability to modulate oxidative stress, regulate Ca<sup>2+</sup>-influx through ion channels, and inhibit apoptosis. Protective mechanism also involves proteins of the Bcl-2 family, the processes of restoration of calcium homeostasis, inhibition of mitochondrial and ER stress pathways, and leading to ultimately to inactivation of caspase-3 and inhibition of apoptosis (Turovsky et al., 2022).

In most neurodegenerative brain tissue disorders, including AD, downregulation of Nrf2 occurred leading to induction of oxidative damaging cascade (Villavicencio Tejo and Quintanilla, 2021). In the current study AlCl<sub>3</sub> administration induced AD, which in turn was coupled with a noticeable enhancement in oxidative stress through hindering Nrf2/HO-1 cue, which is associated with a reduction in TAC and SOD activity and elevation in MDA level in brain tissue. Raising the endogenous defense against free radicals is part of the effective approaches that can halt oxidative stress-mediated neuronal damage (Ramesh and Govindaraju, 2022). Phytochemicals are attractive

therapeutics for the amelioration of AD owing to their actions in impeding oxidative stress and neuroinflammation (Sharifi-Rad et al., 2022a,b).

Liquid chromatography coupled to tandem mass spectrometry (LC-MS/MS) is a crucial technique for characterizing the polyphenol-rich extracts with low noise and high sensitivity (López-Fernández et al., 2020). Polyphenols can be classified into five main categories, including phenolic acids, stilbenes, flavonoids, lignans, and others (Galanakis, 2018). In this study, sixty-six compounds were characterized based on their mass spectra and by comparing to the in-house database and reference literature. Phenolics have immense potential against oxidative stress and represent almost one-third of the aromatic compounds in the human diet (Hollman, 2001). Phenolic and cinnamic acid derivatives have been tentatively identified in *O. corniculata* ME. A class of esters that developed between a quinic acid and certain trans-cinnamic acids, most frequently caffeic, p-coumaric, and ferulic acid is known as chlorogenic acids (CGAs) (Clifford et al., 2006). Herein, we reported the tentative identification of rosmarinic, chlorogenic and caffeoyl quinic acids in addition to others. The conjugation with a hexose (galactose or glucose), pentose (arabinose or xylose), deoxyhexose (rhamnose) and glucuronic acid units is indicated by the neutral loss of 162, 132, 146, 176 mass units, respectively. Meanwhile, the neutral loss of 120 atomic mass unit (amu) (0,2 cross-ring cleavage) and 90 amu (0,3 cross-ring cleavage) denoted the conjugation with C-glycosylation (Cuyckens and Claeys, 2004). Whereas twenty-seven flavonoid structures have been tentatively identified within different classes including flavanone, chalcone, and flavone where flavone and its glycosides represent the main detected compounds (apigenin, apigenin glucuronide, apigenin methyl glucuronide, apigenin hexoside, isovitexin hexoside, vitexin rhamnoside, luteolin, luteolin glucuronide and luteolin hexosylrhamnoside). Besides, many methoxylated flavone have been

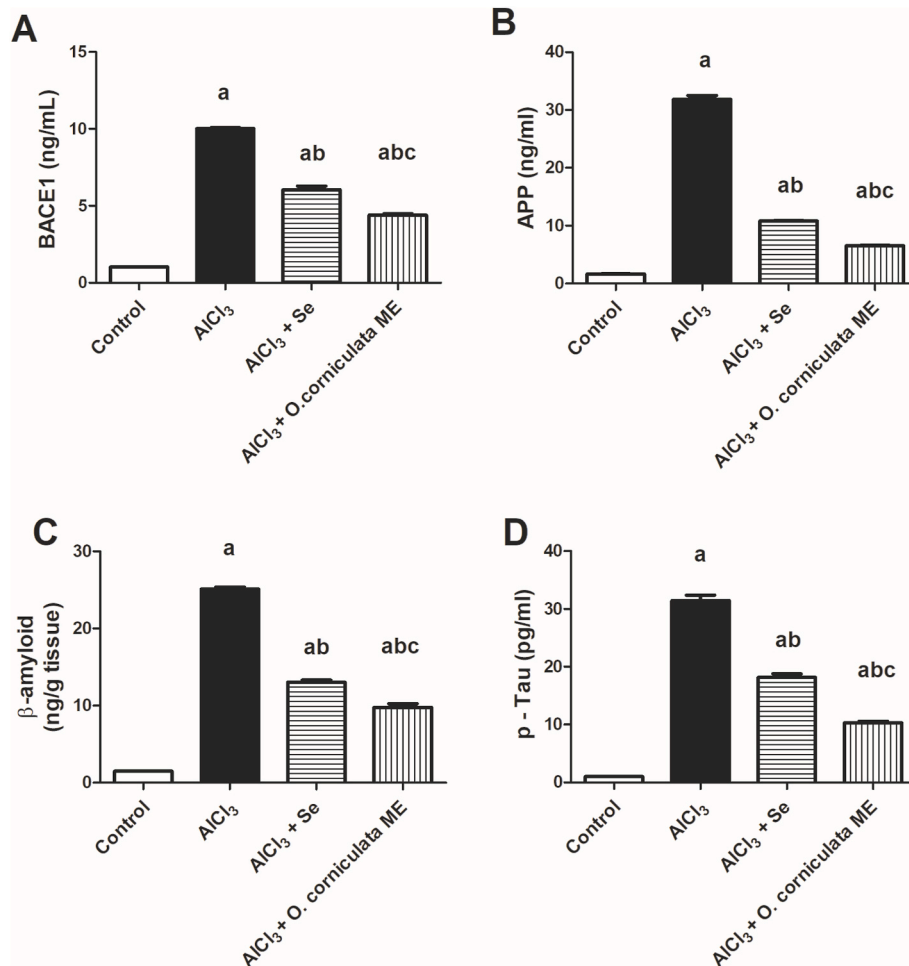


**Fig. 6.** Effect of *O. corniculata* ME and Se on potential AD Biomarkers (BACE1, APP, A $\beta$  Generation, and p-Tau Levels) in Brain Tissue of AlCl<sub>3</sub>-induced AD in Rats. (A) BACE1 level, (B) Brain APP level, (C)  $\beta$ -amyloid level, (D) Brain P-Tau level. <sup>a</sup> Significantly different from control group at  $p < 0.05$ . <sup>b</sup> Significantly different from AlCl<sub>3</sub> group at  $p < 0.05$ . <sup>c</sup> Significantly different from AlCl<sub>3</sub> + Se group.

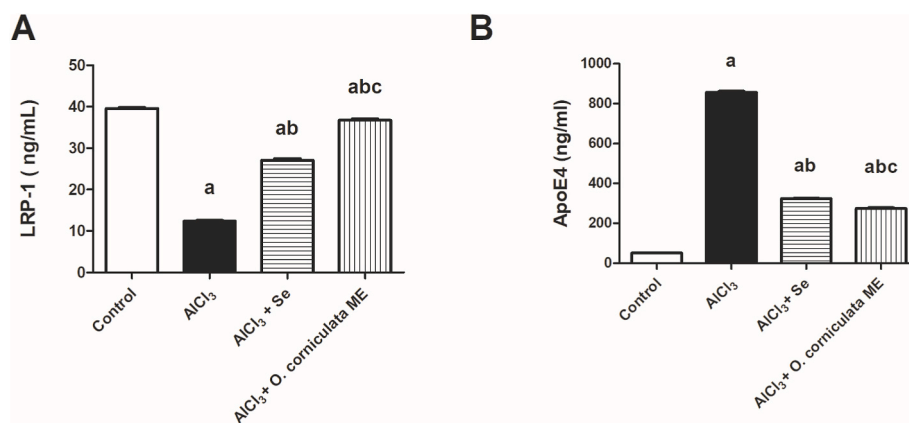


**Fig. 7.** Effect of *O. corniculata* ME and Se Modulation of the Neuronal Receptor; LRP1 and Pathophysiology Biomarker; ApoE4 in Brain tissue of AlCl<sub>3</sub>-induced AD in Rats. (A) LRP-1 level and (B) ApoE4 level. <sup>a</sup> Significantly different from control group at  $p < 0.05$ . <sup>b</sup> Significantly different from AlCl<sub>3</sub> group at  $p < 0.05$ . <sup>c</sup> Significantly different from AlCl<sub>3</sub> + Se group at  $p < 0.05$ .

tentatively identified such as acacetin (methoxy apigenin) and chrysoeriol (methoxylated luteolin).

Based on the results of phytochemical and biochemical analyses, the administration of *O. corniculata* ME reduced the AlCl<sub>3</sub>-stimulated oxidative stress via enhancing Nrf2/HO-1 cue, thereby producing a neuroprotective action endorsed through the amplified monoamine

levels, declined AChE, and amended behavioral and cognitive activities. The previous was confirmed by abridged SAP% in Y-Maze test and enhanced learning and spatial memory in MWM test. In a study performed by Gao et al., *Oxalis corniculata* was established to possess potential antioxidant activity as evidenced by hastening the antioxidant enzymes and dampening the MDA (H. Gao et al., 2022). Apigenin, a

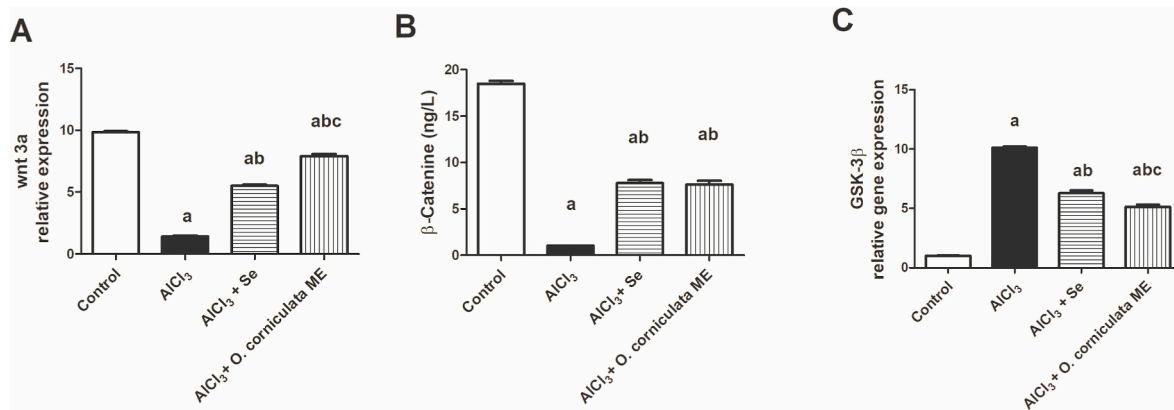


**Fig. 8.** Effect of *O. corniculata* ME and Se on Wnt3a/ $\beta$ -Catenin/GSK3 $\beta$  Pathway in Brain Tissue of AlCl<sub>3</sub>-induced AD in Rats. (A) Wnt3a relative gene expression, (B)  $\beta$ -Catenin level, (C) Brain GSK3 $\beta$  relative gene expression. <sup>a</sup> Significantly different from control group at  $p < 0.05$ . <sup>b</sup> Significantly different from AlCl<sub>3</sub> group at  $p < 0.05$ . <sup>c</sup> Significantly different from AlCl<sub>3</sub> + Se group at  $p < 0.05$ .

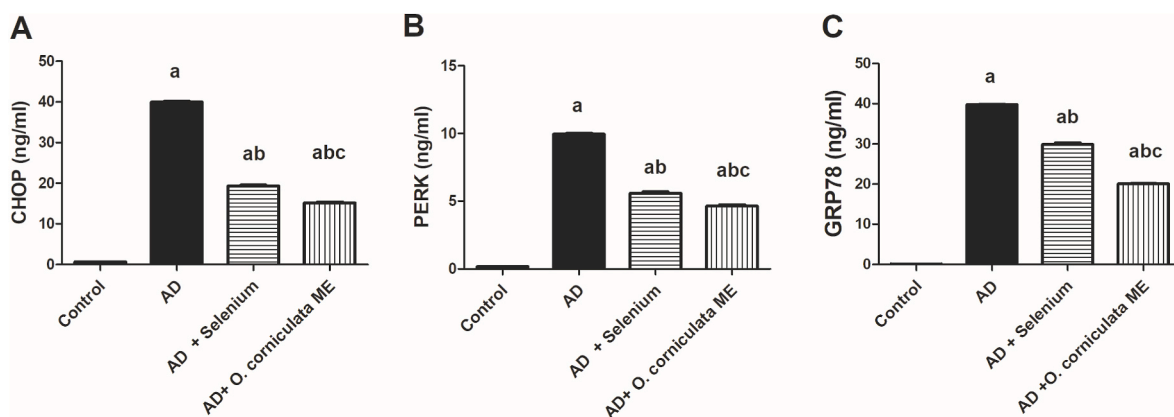


**Fig. 9.** Effect of *O. corniculata* ME and Se on Activation of ER Stress-induced Cell Death Protein; CHOP and UPR Genes; PERK and GRP78 in Brain Tissue of AlCl<sub>3</sub>-induced AD in Rats. (A) CHOP level, (B) PERK level, (C) GRP78 level. <sup>a</sup> Significantly different from control group at  $p < 0.05$ . <sup>b</sup> Significantly different from AlCl<sub>3</sub> group at  $p < 0.05$ . <sup>c</sup> Significantly different from AlCl<sub>3</sub> + Se group at  $p < 0.05$ .

bioactive flavonoid possessing a wide of biological activities, was found in *Oxalis corniculata* ME. In a recent study apigenin administration led to a marked reduction in MDA level and a rise in SOD activity as well as restoration of DA in LPS-induced Parkinson's disease in rats (Patel and Singh, 2022). The polyphenol chlorogenic acid also significantly reduced the level of MDA and prevented the decrease in SOD activity in renal tissue (Bao et al., 2018) and in liver tissue (Shi et al., 2018). The latter conforms to our findings. Another study demonstrated that *O. corniculata* ME contains biologically active phytoconstituents such as phenols, flavonoids, alkaloids, tannins, triterpenes, sterols, and volatile oils. The ethanolic extract showed inhibitory activities against cholinesterase enzyme which may indicate anti-Alzheimer's disease ability (Imran et al., 2020). In the current study, the methanolic extract of *O. corniculata* yielded the bioactive flavonoid isovitexin which exhibited an amelioration in MWM test results in a dose-dependent manner in anesthetic-induced cognitive impairment in rats (Guo et al., 2022) which agrees with our current findings where *O. corniculata* ME enhanced rats performance in MWM test as previously mentioned.

As a result of the alteration of Nrf2/HO-1 pathway and oxidative stress conditions triggered by AlCl<sub>3</sub> administration, the inflammatory surge was generated by elevating NF- $\kappa$ B expression level, thus raising the expression levels of proinflammatory mediators, such as TNF- $\alpha$  and IL-1 $\beta$ , resulting in neuroinflammation in AD (Hamdan et al., 2022; Isaev et al., 2023). Additionally, the release of IL-1 $\beta$  contributes to tau hyperphosphorylation. As mentioned in previous studies, tau is the biomarker for neurofibrillary tangles (NFT) in AD and results in

modifying the stability of the microtubule and axonal transport. When the conformation of tau is modified, this leads to harmful aggregations. Hence, the halting of the accumulation of tau became an attractive approach to halt AD progression (Breijyeh and Karaman, 2020). Moreover, inflammation activates TLR4/NLRP3 axis, resulting in neuroinflammation, the aggregation of A $\beta$  and neurodegeneration (Yang et al., 2020). This finding lends support to ours, since AlCl<sub>3</sub> stimulated TLR4/NLRP3 axis. The initiation of TLR4 interacts with NLRP3 inflammasomes which in turn leads to the activation of caspase-1, releasing IL-1 $\beta$ , which sustains neuroinflammation (Yu et al., 2021). In addition, numerous findings have reported that NLRP3 is closely linked to autophagy (Stancu et al., 2022). The latter is followed by an elevation in the expression level of NF- $\kappa$ B and its associated inflammatory biomarkers, such as TNF- $\alpha$  and IL-1 $\beta$  levels in AD brain relative to normal control rats, which also conforms to previous findings (Hamdan et al., 2022). All the previous data signifies that the TLR4/NLRP3 axis possesses a major part in the pathophysiology of AD. Contrariwise, TLR4 repression can improve learning and memory functions, reduce A $\beta$  accumulation, and control neuronal cell death, consequently eliciting neuroprotection against AD, as mentioned in a study performed by Cui et al. (2020). Ample evidence had documented that phytochemicals can preserve neurons against neurological injuries resulting from the elevated NLRP3 inflammasome via hindering TLR4 signaling hub (Hamdan et al., 2022; Özenver and Efferth, 2021; Spano et al., 2022). These previous data endorse our findings, which showed that *O. corniculata* ME has notably suppressed the inflammatory and

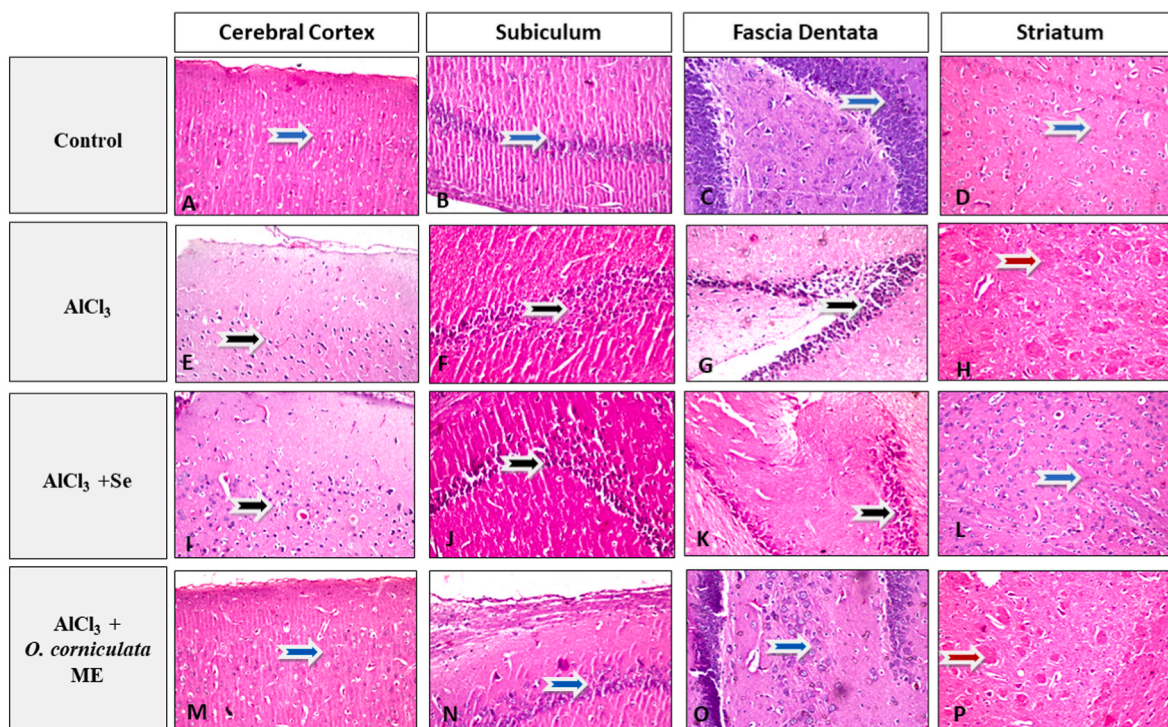


**Fig. 10.** Representative histological section of cerebral tissue specimens stained by H & E (X40). Photomicrographs (A–P): Transverse brain tissue sections from the control group showing no histopathological alteration in the cerebral cortex, hippocampus (Subiculum, Fascia dentata) and striatum.

apoptotic pathways, which were elevated by  $\text{AlCl}_3$  as evidenced by a reduction in TLR4 and NLRP3 expressions when compared with the AD group, showing also better inhibitory effects when compared to rats receiving Se as protective therapy. Moreover, *O. corniculata* ME therapy led to a marked reduction in inflammatory cytokines supported by lessening of  $\text{IL-1}\beta$  and  $\text{TNF-}\alpha$  contents and  $\text{NF-}\kappa\text{B}$  expression. The latter effect might be attributed to the presence of apigenin and acacetin polyphenols in *O. corniculata* ME. Apigenin flavonoid was reported to decrease  $\text{NF-}\kappa\text{B}$  and  $\text{TNF-}\alpha$  release in primary human monocytes and to reduce the expression of  $\text{IL-1}$  (Li et al., 2017) as well as the level of TLR4 (Ginwala et al., 2019). Moreover, apigenin has been reported to reduce the expression of Nrf2 in LPS-induced Parkinson's disease (Patel and Singh, 2022). By the same token, Acacetin was found to reduce  $\text{NF-}\kappa\text{B}$  in sepsis-induced acute lung injury model in mice (Sun et al., 2018). Moreover, Acacetin reduced TAC and nitric oxide production in hepatitis following a renal ischemia/reperfusion model in mice (Jalili et al., 2021). It was also reported by Mancuso et al. (2019) that apigenin and acacetin could inhibit the activation of proinflammatory cytokines and nitric oxide (NO) production, protecting neurons from inflammatory-induced damage in AD. In addition, the flavone isovitexin was reported to reduce  $\text{NF-}\kappa\text{B}$  which in turn deactivates the inflammasome NLRP3 expression as well as  $\text{IL-1}\beta$ ,  $\text{TNF-}\alpha$ , caspase-1 and TLR4 in LPS-induced renal injury (Tseng et al., 2023). Another compound isolated from *O. corniculata* ME is chrysoeriol which was found to reduce neuroinflammation by modulating the expressions of  $\text{NF-}\kappa\text{B}$ ,  $\text{TNF-}\alpha$ ,  $\text{IL-1}\beta$  (Yu et al., 2023). Chlorogenic acid, one of the most plentiful polyphenols isolated from *O. corniculata* ME, possessing known antioxidant and anti-inflammatory features (Jiang et al., 2016). Chlorogenic acid was reported to reduce renal oxidative stress and inflammation in diabetic nephropathy model in rats via activation of Nrf2/HO-1 coupled with its inhibition of  $\text{NF-}\kappa\text{B}$ , as the latter events reinforce each other (Bao et al., 2018). Chlorogenic acid also reduced protein expression of NLRP3, Caspase-1, and  $\text{IL-1}\beta$  in acute liver injury in rats (Shi et al., 2018). In another study performed to test the beneficial effects of chlorogenic acid on the depreciation of inflammation and apoptosis cause by ER stress in rat testes, the polyphenolic compound decreased

the expression of  $\text{TNF}\alpha$ , Bax/Bcl 2 ratio and  $\text{NF-}\kappa\text{B}$  level (Komeili-Movahhed et al., 2023).

Another pathway connected to AD progression is the ApoE4/LRP1 axis. Apolipoprotein E4 (ApoE4) is the strongest predictor for late-onset AD (Na et al., 2023) and its inhibition immensely reduces neuroinflammation and improves tauopathy. Therefore, ApoE4 depletion is a promising way for the management of AD (X. Li et al., 2022; Y. Li et al., 2022). Key physiological functions of ApoE4 are mediated by LRP1 which acts as a scavenger of damaging waste products from the brain, especially amyloid beta ( $\text{A}\beta$ ). Hence, LRP1 is becoming an increasingly important object of research as well (Barić, 2022) since the reduction in LRP1 levels had been documented in AD etiopathology (Li et al., 2020; Shinohara et al., 2017). However, ApoE4 competes and has a higher binding affinity for LRP1 at the glial cells and neuronal surface, halting  $\text{A}\beta$  clearance resulting in its accumulation, which promotes the formation of senile plaques (Pires and Rego, 2023; Zhang et al., 2019). In the current study,  $\text{AlCl}_3$  treatment increased ApoE4 level while LRP1 level was reduced relative to the untreated group (i.e., control group), which confirms the notion that long time exposure to aluminum is able to aggravate AD prognosis via stimulation of ApoE4/LRP1. Nevertheless, *O. corniculata* ME administration intervenes with the effect of  $\text{AlCl}_3$  in changing ApoE4 and LRP1 expressions. Mountaki et al. (2021) studied the effect of phytochemicals on AD-related functions of ApoE4 forms and found that polar phenols can alter the arrangement of ApoE4 and halt the deleterious actions of ApoE4 on AD progression (Mountaki et al., 2021).

Research investigating the effect of the major isolated compounds from *O. corniculata* ME, such as apigenin, acacetin, luteolin, chlorogenic acid, isovitexin and chrysoeriol on ApoE4/LRP1 axis are scarce. However, a study performed by Zhang et al. (2023), reported that luteolin has a strong binding affinity to LRP1 and that the therapeutic effects of luteolin were regulated by LRP1 which in turn mitigates the expression of inflammation-related protein matrix metalloproteinase-9 (MMP9) in autism spectrum disorder patients (Zhang et al., 2023).

Additionally, alteration of Wnt 3/ $\beta$ -catenin/GSK-3 $\beta$  pathway is related to the pathophysiology of neurodegenerative diseases (Liu et al.,

2019). GSK-3 $\beta$  disruption is linked to AD's etiology and A $\beta$ -induced neurotoxicity since it is involved in Tau phosphorylation (You et al., 2022). Consequently, it is considered beneficial to inhibit GSK-3 $\beta$  to prevent neurodegeneration and AD (Lee et al., 2022). Interestingly, *O. corniculata* ME repaired the decrement of Wnt3a, and  $\beta$ -catenin produced via AlCl<sub>3</sub>. On the other hand, GSK-3 $\beta$  was markedly prohibited due to *O. corniculata* ME therapy. Thereby, the elevation of Wnt3/ $\beta$ -catenin cue suppresses the production of A $\beta$  production and the hyperphosphorylation of tau protein (Jia et al., 2019; J. Liu et al., 2022), in addition to enhancing BDNF level, pivotal in controlling neuronal plasticity and mending learning and memory functions by improving central cholinergic neurotransmission and hence guards against a variety of neurodegenerative ailments through augmenting endogenous antioxidant systems (Abbas et al., 2022). Luteolin found in *O. corniculata* ME was reported to induce the down-regulation of TNF- $\alpha$  expression, along with interleukins and chemokines, in addition to reducing oxidative stress by scavenging ROS and regulating transcription factors such as CREB, NF-K $\beta$  and  $\beta$ -catenin (Ali and Siddique, 2019). In a study performed on AD rat model, apigenin significantly attenuated the hyperphosphorylation of tau in the brain moreover RT-PCR Real-time PCR showed notable reduction of BACE1 and GSK-3 $\beta$  (Alsadat et al., 2021) which agrees with our findings.

It was previously suggested that autophagy impairment is linked to the pathophysiology of neurodegenerative diseases, including AD. Atypical protein accumulation give rise to synaptic dysfunction and neuronal degeneration, clearing such anomalous protein accumulation is vital aim for the amelioration of these maladies. Autophagy is necessary to clear the protein aggregations in neurons and hence hinders apoptosis (L. Liu et al., 2022). Beclin-1 is a well-known autophagy inducer that controls the initiation of autophagosome formation (Pang et al., 2022). The present study showed that *O. corniculata* ME treatment promoted autophagy by increasing the level of beclin-1 which may be due to its apigenin content. Recently, apigenin was reported to aid autophagy by up-regulating beclin-1 (Liang et al., 2023). Another significant compound isovitexin showed improvement in a sevoflurane-induced cognitive dysfunction model in rats via modulating autophagy in brain through enhancing of Beclin-1 (Guo et al., 2022).

AlCl<sub>3</sub> administration generated apoptosis as evidenced by the reduction of anti-apoptotic *Bcl-2* and the elevation in the apoptotic *Bax* expression hence elevating *Bax/Bcl-2* ratio. Apoptosis is a leading pathway of cell death during AD (Naseri et al., 2022). Besides, our findings pointed to that *O. corniculata* ME slowed apoptosis by upregulation of *Bcl-2* expression level and downregulation of the *Bax* expression level and reversing the *Bax/Bcl-2* ratio in AlCl<sub>3</sub> treated rats.

It is important to note that autophagy and apoptosis are two diverse procedures. Autophagy can create an advantageous environment for cells' survival. Also, autophagy hinders endoplasmic reticulum (ER) stress by degrading misfolded protein accumulations and hence prevents the upregulation of the UPR (Unfolded Protein Response) (Pang et al., 2022). In ER, the UPR is a quality control machinery, where the cell tries to preserve homeostasis (Hughes and Mallucci, 2019). Failure in maintaining homeostasis activates apoptosis (Andreone et al., 2020). As previously mentioned, AD had been associated to increasing the level of phosphorylated Tau protein (pTau), resulting in accumulation of neurofibrillary tangles (NFT) inside the neuronal cells, and accumulation of plaques outside the neuronal via accumulation of A $\beta$  peptides, due to chromosomal alterations in the amyloid precursor protein (APP) (Guo et al., 2020; Sasaguri et al., 2022). The latter were shown to inhibit ER-associated degradation pathway (ERAD) and the proteasome machinery (Shacham et al., 2021) thus encouraging ER stress and stimulating UPR (Montibeller and De Bellerocche, 2018). PERK, and beta-site APP cleaving enzyme 1 (BACE1) have been found to be upregulated in AD. The PERK axis presents a crucial part in the integrated stress response which conserves intracellular signaling network (Shacham et al., 2021). The sustained PERK stimulation in AD was reported to negatively impact memory and enhance neurodegeneration (Ohno,

2018).

Under prolonged ER stress, AD brain showed upregulation in the expression of the pro-apoptotic gene CHOP as well as increased levels of GRP78 and PERK inducing UPR, which in turn precipitates oxidative stress induction which further leads to A $\beta$  accumulation resulting in neuronal death (Casas, 2017; T. Gao et al., 2022; Lee et al., 2010; Y. Li et al., 2022).

The protective effect of acacetin, identified in *O. corniculata* ME, on A $\beta$  production is mediated by transcriptional regulation of BACE-1 and APP, resulting in decreased APP protein expression and synthesis resulting in a decrease in the number of amyloid plaques in addition to BACE-1 activity (Wang et al., 2015). Literature also mentioned that isovitexin was found to activate BDNF hence preventing senile cognitive impairment caused by aging (Azimi et al., 2018) which conforms to our findings.

AlCl<sub>3</sub> administration resulted in a marked rise in PERK, GRP78, and CHOP expressions in rats' brain which conforms to previous studies where AlCl<sub>3</sub> resulted in ER stress mediated by CHOP overexpression in AlCl<sub>3</sub> (Khalaf et al., 2022) induced testicular damage. In another study, it was observed that aluminum potentially enhanced protein levels of PERK, indicating that aluminum mediated UPR stimulation via ER stress leading to the switching on of the inflammatory and apoptotic pathways (Rizvi et al., 2016). On the other hand, *O. corniculata* ME demonstrated a reduction in PERK, GRP78, and CHOP expressions in rats treated with AlCl<sub>3</sub> suggesting that *O. corniculata* ME can provide neuroprotection through inhibition of apoptosis and autophagy promotion. It was reported that acacetin was found to reduce the expression of endoplasmic reticulum stress markers CHOP and PERK, as well as apoptosis related *Bax* in a dose dependent manner (Miao et al., 2023) which conforms to the findings in the study at hand. Furthermore, *O. corniculata* ME exhibited an amelioration *Bcl-2* gene expression and a marked reduction in the gene expression of *Bax* compared to AlCl<sub>3</sub> treated rats which might be attributed to the presence of another flavonoid, isovitexin. The latter compound was found to cause significant reduction in *Bax* and a notable rise in *Bcl-2*. The previous findings corroborate the fact that *O. Corniculata* inhibits AlCl<sub>3</sub>-induced brain apoptosis and promotes autophagy AD in rats.

## 5. Conclusion

In this work, the role of Se or *O. corniculata* ME, to enhance behavioral and biochemical function in the AlCl<sub>3</sub> treated brain, was investigated. Moreover, our findings demonstrated that *O. corniculata* ME has a potential superior role compared to Se in preventing AD by modulating various axes, particularly Nrf2/HO-1, TLR4/NLRP3, APOE4/LRP1, and Wnt 3/ $\beta$ -catenin/GSK-3 $\beta$  and PERK cues. The potential effects of *O. corniculata* in controlling AD may be mediated by the phenolic compounds isolated from its methanolic extract contributing to its neuroprotective effect which might be explained by the synergistic effects found among the compounds as well as their potent antioxidant, anti-inflammatory and anti-apoptotic action, hence protecting neurons.

## Funding

This research received no specific grant from funding agencies in the public, commercial, or not-for-profit sectors.

## Informed consent statement

Not applicable.

## Institutional review board statement

In accordance with the guidelines of the Guide for Care and Use Laboratory Animals, published by the National Institutes of Health (NIH Publications No. 8023, revised 1978) and the ARRIVE criteria, all

animal procedures and experimental methods used in the current study were approved by the Animal care and use committee of the Faculty of Pharmacy, Al-Azhar University (Ethical approval No. 371/2023).

#### Informed consent statement

Not applicable.

#### CRediT authorship contribution statement

**Karema Abu-Elfotuh:** Writing – review & editing, Writing – original draft, Methodology, Formal analysis, Data curation, Conceptualization. **Ahmed M.E. Hamdan:** Writing – review & editing, Methodology, Formal analysis, Data curation. **Shaza A. Mohamed:** Writing – review & editing, Writing – original draft, Methodology, Formal analysis, Data curation. **Riham O. Bakr:** Writing – review & editing, Writing – original draft, Methodology, Formal analysis, Data curation. **Amal H. Ahmed:** Writing – review & editing, Writing – original draft, Formal analysis, Data curation. **Ahmed M. Atwa:** Writing – review & editing, Formal analysis, Data curation. **Amira M. Hamdan:** Writing – review & editing, Formal analysis, Data curation. **Ahad Ghanem Alanzai:** Writing – review & editing, Formal analysis, Data curation. **Raghad Khalid Alnahhas:** Writing – review & editing, Formal analysis, Data curation. **Ayah M.H. Gowifel:** Writing – review & editing, Writing – original draft, Methodology, Formal analysis, Data curation. **Maha A. Salem:** Writing – review & editing, Writing – original draft, Methodology, Formal analysis, Data curation.

#### Declaration of competing interest

The authors declare that they have no known competing financial interests or personal relationships that could have appeared to influence the work reported in this paper.

#### Data availability

Data will be made available on request.

#### Abbreviations

AD	Alzheimer's disease
AlCl <sub>3</sub>	Aluminum chloride
Aβ	Amyloid beta-peptide
DA	Dopamine
ACHE	Acetylcholine esterase
NE	Norepinephrine
5 H T	Serotonin
BDNF	Brain-derived neurotrophic factor, associated X protein
Bcl-2	B-cell lymphoma-2 protein
GSK-3β	Glycogen synthase kinase-3β
Bax	B-cell lymphoma protein 2
IL-1β	Interleukin-1β
NF-κB	Nuclear factor kappa B
TNF-α	Tumor necrosis factor alpha
LRP1	low density lipoprotein receptor-related protein 1
p.o	Orally
MDA	Malondialdehyde
TLR-4	Toll-like receptor-4
SOD	Superoxide dismutase
Nrf2/HO-1	Nuclear factor erythroid 2-related factor 2/hemoxygenase-1
NLRP3	NLR family pyrin domain containing 3
CHOP	C/EBP homologous binding protein
p-PERK	Phospho-protein kinase R-like endoplasmic reticulum kinase
GRP78	Glucose-regulated protein 78
BECLIN1	Bcl-2-homology (BH)-3 domain

Se Selenium

#### Appendix A. Supplementary data

Supplementary data to this article can be found online at <https://doi.org/10.1016/j.jep.2024.117731>.

#### References

- Abbas, F., Eladl, M.A., El-Sherbiny, M., Abozied, N., Nabil, A., Mahmoud, S.M., Mokhtar, H.I., Zaitone, S.A., Ibrahim, D., 2022. Celastrol and thymoquinone alleviate aluminum chloride-induced neurotoxicity: behavioral psychomotor performance, neurotransmitter level, oxidative-inflammatory markers, and BDNF expression in rat brain. *Biomed. Pharmacother.* 151, 113072.
- Abhilash, P., Nisha, P., Prathapan, A., Nampootheri, S.V., Cherian, O.L., Sunitha, T., Raghu, K., 2011. Cardioprotective effects of aqueous extract of *Oxalis corniculata* in experimental myocardial infarction. *Exp. Toxicol. Pathol.* 63 (6), 535–540.
- Abu-Elfotuh, K., Ragab, G.M., Salahuddin, A., Jamil, L., Abd Al Haleem, E.N., 2021. Attenuative effects of fluoxetine and Triticum aestivum against aluminum-induced alzheimer's disease in rats: the possible consequences on hepatotoxicity and nephrotoxicity. *Molecules* 26 (21), 6752.
- Ahmad, F., Sachdeva, P., 2022. Critical appraisal on mitochondrial dysfunction in Alzheimer's disease. *Aging Med* 5 (4), 272–280.
- Al-Qalhati, I.R.S., Waly, M., Al-Attabi, Z., Al-Subhi, L.K., 2016. Protective effect of Pteropyrum scoparium and *Oxalis corniculata* against streptozotocin-induced diabetes in rats. *Faseb. J.* 30, 1176.1174-1176.1174.
- Ali, A.A., Ahmed, H.I., Abu-Elfotuh, K., 2016. Modeling stages mimic Alzheimer's disease induced by different doses of aluminum in rats: focus on progression of the disease in response to time. *J Alzheimer's Parkinsonism Dementia* 1 (1), 2.
- Ali, F., Siddique, Y.H., 2019. Bioavailability and pharmacotherapeutic potential of luteolin in overcoming Alzheimer's disease. *CNS Neurol. Disord.: Drug Targets* 18 (5), 352–365.
- Alsadat, A.M., Nikbakht, F., Nia, H.H., Golab, F., Khadem, Y., Barati, M., Vazifekah, S., 2021. GSK-3β as a target for apigenin-induced neuroprotection against Aβ 25–35 in a rat model of Alzheimer's disease. *Neuropeptides* 90, 102200.
- Andreone, B.J., Larhammar, M., Lewcock, J.W., 2020. Cell death and neurodegeneration. *Cold Spring Harbor Perspect. Biol.* 12 (2), a036434.
- Aruna, K., Devi, P., Rajeswari, R., Sankar, S.R., 2017. The effect of *Oxalis corniculata* extract against the behavioral changes induced by 1-methyl-4-phenyl-1,2,3,6-tetrahydropyridine (MPTP) in mice. *J. Appl. Pharmaceut. Sci.* 7 (3), 148–153.
- Aruna, K., Rajeswari, P.D.R., Sankar, S.R., 2016. The effects of *Oxalis corniculata* L. extract against MPTP induced oxidative stress in mouse model of Parkinson's disease. *J. Pharmaceut. Sci. Res.* 8 (10), 1136.
- Azimi, M., Gharakhanlou, R., Naghdi, N., Khodadadi, D., Heysieattalab, S., 2018. Moderate treadmill exercise ameliorates amyloid-beta-induced learning and memory impairment, possibly via increasing AMPK activity up-regulation of the PGC-1 alpha/FNDC5/BDNF pathway. *Peptides* 102, 78–88.
- Bakr, R.O., Mohamed, S.A.E.H., Ayoub, N., 2016. Phenolic profile of *Centaurea aegyptiaca* L. growing in Egypt and its cytotoxic and antiviral activities. *Afr. J. Tradit., Complementary Altern. Med.* 13 (6), 135–143, 29.
- Bancroft, J.D., Gamble, M., 2008. *Theory and Practice of Histological Techniques*, sixth ed. Churchill Livingstone, Elsevier, China.
- Bao, L., Li, J., Zha, D., Zhang, L., Gao, P., Yao, T., Wu, X., 2018. Chlorogenic acid prevents diabetic nephropathy by inhibiting oxidative stress and inflammation through modulation of the Nrf2/HO-1 and NF-κB pathways. *Int. Immunopharm.* 54, 245–253.
- Barić, N., 2022. The decline of the expression of low density lipoprotein receptor-related protein 1 (LRP1) during normal ageing and in Alzheimer's disease. *Glycative Stress Res* 9 (2), 42–54.
- Breijyeh, Z., Karaman, R., 2020. Comprehensive review on alzheimer's disease: causes and treatment. *Molecules* 25 (24), 5789.
- Cano, A., Turowski, P., Ettcheto, M., Duskey, J.T., Tosi, G., Sánchez-López, E., García, M. L., Camins, A., Souto, E.B., Ruiz, A., 2021. Nanomedicine-based technologies and novel biomarkers for the diagnosis and treatment of Alzheimer's disease: from current to future challenges. *J.Nanobiotechnology* 19 (1), 1–30.
- Casas, C., 2017. GRP78 at the centre of the stage in cancer and neuroprotection. *Front. Neurosci.* 11, 77.
- Clifford, M.N., Zheng, W., Kuhnert, N., 2006. Profiling the chlorogenic acids of aster by HPLC. *MSn. Phytochem. Anal.* 17 (6), 384–393.
- Cui, W., Sun, C., Ma, Y., Wang, S., Wang, X., Zhang, Y., 2020. Inhibition of TLR4 induces M2 microglial polarization and provides neuroprotection via the NLRP3 inflammasome in Alzheimer's disease. *Front. Neurosci.* 14, 444.
- Cuyckens, F., Claeys, M., 2004. Mass spectrometry in the structural analysis of flavonoids. *J. Mass Spectrom.* 39 (1), 1–15.
- Das, M., Gohain, K., 2018a. Evaluation of memory enhancing activity of methanolic extract of *Oxalis corniculata* Linn on Dementia in experimental animals. *Int. J. Sci. Eng. Res.* 9 (3), 922–928.
- Das, M., Gohain, K., 2018b. Study of neuroprotective activity of methanolic extract of *Oxalis corniculata* linn on animal models of depression. *Int. J. Eng. Sci. Res. Technol.* 7 (6), 397–405.
- Dighe, S.B., Kuchekar, B., Wankhede, S., 2016. Analgesic and anti-inflammatory activity of β-sitosterol isolated from leaves of *Oxalis corniculata*. *Int. J. Pharmacol. Res.* 6, 109–113.

- Elbini-dhoubi, I., Doghri, R., Ellefi, A., Degraç, I., Srairi-Abid, N., Gati, A., 2021. Curcumin attenuated neurotoxicity in sporadic animal model of Alzheimer's disease. *Molecules* 26 (10), 3011.
- Galanakis, C.M., 2018. Polyphenols: Properties, Recovery, and Applications. Woodhead Publishing.
- Gao, H., Lei, X., Ye, S., Ye, T., Hua, R., Wang, G., Song, H., Zhou, P., Wang, Y., Cai, B., 2022. Genistein attenuates memory impairment in Alzheimer's disease via ERS-mediated apoptotic pathway in vivo and in vitro. *J. Nutr. Biochem.* 109, 109118.
- Gao, F., Zhao, J., Liu, P., Ji, D., Zhang, L., Zhang, M., Li, Y., Xiao, Y., 2020. Preparation and in vitro evaluation of multi-target-directed selenium-chondroitin sulfate nanoparticles in protecting against the Alzheimer's disease. *Int. J. Biol. Macromol.* 142, 265–276.
- Gao, T., Hu, W., Zhang, Z., Tang, Z., Chen, Y., Zhang, Z., Yuan, S., Chen, T., Huang, Y., Feng, S., 2022. An acidic polysaccharide from *Oxalis corniculata* L. and the preliminary study on its antioxidant activity. *J. Food Biochem.* 46 (9), e14235.
- Giacobini, E., Cuello, A.C., Fisher, A., 2022. Reimagining cholinergic therapy for Alzheimer's disease. *Brain* 145 (7), 2250–2275.
- Ginwala, R., Bhavsar, R., Chigbu, D.G.I., Jain, P., Khan, Z.K., 2019. Potential role of flavonoids in treating chronic inflammatory diseases with a special focus on the anti-inflammatory activity of apigenin. *Antioxidants* 8 (2), 35.
- Guo, T., Zhang, D., Zeng, Y., Huang, T.Y., Xu, H., Zhao, Y., 2020. Molecular and cellular mechanisms underlying the pathogenesis of Alzheimer's disease. *Mol. Neurodegener.* 15 (1), 1–37.
- Guo, Y., Chen, Q., Wu, B., Sun, L., 2022. Isovexitin restores sevoflurane-induced cognitive dysfunction by mediating autophagy through activation of the PGC-1 $\alpha$ /FNDC5 signaling pathway. *Acta Neurobiol. Exp.* 82 (3), 373–379.
- Gupta, P., Bajpai, S.K., Chandra, K., Singh, K.L., Tandon, J.S., 2005. Antiviral profile of Nycnantes arbortristis L. against encephalitis causing viruses. *Indian J. Exp. Biol.* 43 (12), 1156–1160.
- Hamdan, A.M.E., Alharthi, F.H.J., Alanazi, A.H., El-Emam, S.Z., Zaghlool, S.S., Metwally, K., Albalawi, S.A., Abdu, Y.S., Mansour, R.E.-S., Salem, H.A., 2022. Neuroprotective effects of phytochemicals against aluminum chloride-induced Alzheimer's disease through ApoE4/LRP1, wnt 3/ $\beta$ -catenin/gsk3 $\beta$ , and TLR4/NLRP3 pathways with physical and mental activities in a rat model. *Pharmaceuticals* 15 (8), 1008.
- Han, X., 2016. In: Lipidomics, X. Han (Ed.), Fragmentation Patterns of Fatty Acids and Modified Fatty Acids. John Wiley & Sons.
- Hegazy, M.M., Metwaly, A.M., Mostafa, A.E., Radwan, M.M., Mehany, A.B., Ahmed, E., Enany, S., Magdeldin, S., Afifi, W.M., ElSohly, M.A., 2021. Biological and chemical evaluation of some African plants belonging to Kalanchoe species: antitypanosomal, cytotoxic, antipolisomerase I activities and chemical profiling using ultra-performance liquid chromatography/quadrupole-time-of-flight mass spectrometer. *Phcog. Mag.* 17 (73), 6–15.
- Herrero, A., Barja, G., 2000. Localization of the site of oxygen radical generation inside the complex I of heart and nonsynaptic brain mammalian mitochondria. *J. Bioenerg. Biomembr.* 32, 609–615.
- Hollman, P.C.H., 2001. Evidence for health benefits of plant phenols: local or systemic effects? *J. Sci. Food Agric.* 81 (9), 842–852.
- Hossain, R., Quispe, C., Saikat, A.S.M., Jain, D., Habib, A., Janmeda, P., Islam, M.T., Radha, Daştan, S.D., Kumar, M., Butnariu, M., Cho, W.C., Sharifi-Rad, J., Kipchakbayeva, A., Calina, D., 2022a. Biosynthesis of secondary metabolites based on the regulation of MicroRNAs. *BioMed Res. Int.* 2002, 9349897.
- Hossain, R., Sarkar, C., Hassan, S.M.H., Khan, R.A., Arman, M., Ray, P., Islam, M.T., Daştan, S.D., Sharifi-Rad, J., Almarhoon, Z.M., Martorell, M., Setzer, W.N., Calina, D., 2022b. In silico screening of natural products as potential inhibitors of SARS-CoV-2 using molecular docking simulation. *Chin. J. Integr. Med.* 28 (3), 249–256.
- Hughes, D., Mallucci, G.R., 2019. The unfolded protein response in neurodegenerative disorders—therapeutic modulation of the PERK pathway. *FEBS J.* 286 (2), 342–355.
- Hukkeri, V., Akki, K., Sureban, R., Gopalkrishnan, B., Byahatti, V., Rajendra, S., 2006. Hepatoprotective activity of the leaves *Oxalis corniculata* Linn. *Indian J. Pharmaceut. Sci.* 4, 542–543.
- Ibrahim, M., Hussain, I., Imran, M., Hussain, N., Hussain, A., Mahboob, T., 2013. Corniculatin A, a new flavonoidal glucoside from *Oxalis corniculata*. *Rev. bras. Farmacogn.* 23 (4), 630–634.
- Imran, M., Irfan, A., Ibrahim, M., Assiri, M.A., Khalid, N., Ullah, S., Al-Sehemi, A.G., 2020. Carbonic anhydrase and cholinesterase inhibitory activities of isolated flavonoids from *Oxalis corniculata* L. and their first-principles investigations. *Ind. Crops Prod.* 148, 112285.
- Isaev, N.K., Genrikhs, E.E., Stelmashook, E.V., 2023. Antioxidant thymoquinone and its potential in the treatment of neurological diseases. *Antioxidants* 12 (2), 433.
- Jain, B.J., Mohd, A.F., Varun, J., 2023. An evidence-based ethnomedicinal study on *Oxalis corniculata*: review of decade study Vibhor Kumar. *Int. J. Green Pharm.* 17 (1), 1–11.
- Jalili, C., Akhshi, N., Raissi, F., Shiravi, A., Alvani, A., Vaezi, G., Nedaei, S.E., Ghanbari, A., 2021. Acacetin alleviates hepatitis following renal ischemia–reperfusion in male Balb/C mice by antioxidants regulation and inflammatory markers suppression. *J. Invest. Surg.* 34 (5), 495–503.
- Jeremic, D., Jiménez-Díaz, L., Navarro-López, J.D., 2021. Past, present and future of therapeutic strategies against amyloid- $\beta$  peptides in Alzheimer's disease: a systematic review. *Ageing Res. Rev.* 72, 101496.
- Jia, L., Piña-Crespo, J., Li, Y., 2019. Restoring Wnt/ $\beta$ -catenin signaling is a promising therapeutic strategy for Alzheimer's disease. *Mol. Brain* 12, 1–11.
- Jiang, R., Hodgson, J.M., Mas, E., Croft, K.D., Ward, N.C., 2016. Chlorogenic acid improves ex vivo vessel function and protects endothelial cells against HOCl-induced oxidative damage, via increased production of nitric oxide and induction of HmoX-1. *J. Nutr. Biochem.* 27, 53–60.
- Kabach, I., Bouchmaa, N., Zouaoui, Z., Ennoury, A., El Asri, S., Laabar, A., Oumeslakht, L., Cacciola, F., El Majdoub, Y.O., Mondello, L., Zyad, A., 2023. Phytochemical profile and antioxidant capacity,  $\alpha$ -amylase and  $\alpha$ -glucosidase inhibitory activities of *Oxalis pes-caprae* extracts in alloxan-induced diabetic mice. *Biomed. Pharmacother.* 160, 114393.
- Khalaf, H.A., Elsamandouy, A.Z., Abo-Elkhair, S.M., Hassan, F.E., Mohie, P.M., Ghoneim, F.M., 2022. Endoplasmic reticulum stress and mitochondrial injury are critical molecular drivers of AIC3-induced testicular and epididymal distortion and dysfunction: protective role of taurine. *Histochem. Cell Biol.* 158 (1), 97–121.
- Khalil, H.M., Azouz, R.A., Hozyen, H.F., Aljuaydi, S.H., AbuBakr, H.O., Emam, S.R., Al-Mokaddem, A.K., 2022. Selenium nanoparticles impart robust neuroprotection against deltamethrin-induced neurotoxicity in male rats by reversing behavioral alterations, oxidative damage, apoptosis, and neuronal loss. *Neurotoxicology* 91, 329–339.
- Khare, C., 2007. *Indian Medicinal Plants: An Illustrated Dictionary*. Springer-Verlag, Berlin pp. 699–700.
- Komeili-Movahhed, T., Heidari, F., Moslehi, A., 2023. Chlorogenic acid alleviated testicular inflammation and apoptosis in tunicamycin induced endoplasmic reticulum stress. *Phys. Int.* 110 (1), 19–33.
- Kumar, K.S., Suthakaran, R., Bairam, R., 2018. Influence of dietary substances on recognition memory in Albino mice. *Res. j. pahrmaol. pharmacodyn.* 10 (4), 156–158.
- Lakshmi, B.V.S., Sudhakar, M., Prakash, K.S., 2015. Protective effect of selenium against aluminum chloride-induced Alzheimer's disease: behavioral and biochemical alterations in rats. *Biol. Trace Elem. Res.* 165, 67–74.
- Liang, Y., Zhong, Q., Ma, R., Ni, Z., Thakur, K., Zhang, J., Wei, Z., 2023. Apigenin, a natural flavonoid, promotes autophagy and ferroptosis in human endometrial carcinoma Ishikawa cells in vitro and in vivo. *Food Sci. Hum. Wellness* 12 (6), 2242–2251.
- Lee, J.H., Won, S.M., Suh, J., Son, S.J., Moon, G.J., Park, U.-J., Gwag, B.J., 2010. Induction of the unfolded protein response and cell death pathway in Alzheimer's disease, but not in aged Tg2576 mice. *Exp. Mol. Med.* 42 (5), 386–394.
- Lee, Y., Bortolotto, Z.A., Bradley, C.A., Sanderson, T.M., Zhuo, M., Kaang, B.-K., Collingridge, G.L., 2022. The GSK-3 inhibitor CT99021 enhances the acquisition of spatial learning and the accuracy of spatial memory. *Front. Mol. Neurosci.* 14.
- Li, F., Lang, F., Zhang, H., Xu, L., Wang, Y., Zhai, C., Hao, E., 2017. Apigenin alleviates endotoxin-induced myocardial toxicity by modulating inflammation, oxidative stress, and autophagy. *Oxid. Med. Cell. Longev.* 2017, 2302896.
- Li, S., Long, C., Liu, F., Lee, S., Guo, Q., Li, R., Liu, Y., 2006. Herbs for medicinal baths among the traditional Yao communities of China. *J. Ethnopharmacol.* 108 (1), 59–67.
- Li, X., Qin, Y., Ye, S., Song, H., Zhou, P., Cai, B., Wang, Y., 2022. Protective effect of Huangpu Tongqiao capsule against Alzheimer's disease through inhibiting the apoptosis pathway mediated by endoplasmic reticulum stress in vitro and in vivo. *Saudi Pharmaceut. J.* 30 (11), 1561–1571.
- Li, Y., Macyczko, J.R., Liu, C.-C., Bu, G., 2022. ApoE4 reduction: an emerging and promising therapeutic strategy for Alzheimer's disease. *Neurobiol. Aging* 115, 20–28.
- Li, Y., Zhang, J., Wan, J., Liu, A., Sun, J., 2020. Melatonin regulates A $\beta$  production/clearance balance and A $\beta$  neurotoxicity: a potential therapeutic molecule for Alzheimer's disease. *Biomed. Pharmacother.* 132, 110887.
- Liu, D., Chen, L., Zhao, H., Vaziri, N.D., Ma, S.-C., Zhao, Y.-Y., 2019. Small molecules from natural products targeting the Wnt/ $\beta$ -catenin pathway as a therapeutic strategy. *Biomed. Pharmacother.* 117, 108990.
- Liu, J., Xiao, Q., Xiao, J., Niu, C., Li, Y., Zhang, X., Zhou, Z., Shu, G., Yin, G., 2022. Wnt/ $\beta$ -catenin signalling: function, biological mechanisms, and therapeutic opportunities. *Signal Transduct. Targeted Ther.* 7 (1), 3.
- Liu, L., Dai, W.-Z., Zhu, X.-C., Ma, T., 2022. A review of autophagy mechanism of statins in the potential therapy of Alzheimer's disease. *J. Integr. Neurosci.* 21 (2).
- Liu, W., Kong, Y., Zu, Y., Fu, Y., Luo, M., Zhang, L., Li, J., 2010. Determination and quantification of active phenolic compounds in pigeon pea leaves and its medicinal product using liquid chromatography–tandem mass spectrometry. *J. Chromatogr. A* 1217, 4723–4731.
- Livak, K.J., Schmittgen, T.D., 2001. Analysis of relative gene expression data using real-time quantitative PCR and the 2 $^{-\Delta\Delta CT}$  method. *Methods* 25 (4), 402–408.
- López-Fernández, O., Domínguez, R., Pateiro, M., Munekata, P.E., Rocchetti, G., Lorenzo, J.M., 2020. Determination of polyphenols using liquid chromatography–tandem mass spectrometry technique (LC–MS/MS): a review. *Antioxidants* 9 (6), 479.
- Mancuso, R., Sicurella, M., Agostini, S., Marconi, P., Clerici, M., 2019. Herpes simplex virus type 1 and Alzheimer's disease: link and potential impact on treatment. *Expert Rev. Anti-infect. Ther.* 17 (9), 715–731.
- Mehrbeheshti, N., Esmaili, Z., Ahmadi, M., Moosavi, M., 2022. A dose response effect of oral aluminum nanoparticle on novel object recognition memory, hippocampal caspase-3 and MAPKs signaling in mice. *Behav. Brain Res.* 417, 113615.
- Miao, J., Yao, S., Sun, H., Jiang, Z., Gao, Z., Xu, J., Chen, K., 2023. Protective effect of water-soluble acacetin prodrug on APAP-induced acute liver injury is associated with upregulation of PPAR $\gamma$  and alleviation of ER stress. *Int. J. Mol. Sci.* 24 (14), 11320.
- Mizokami, H., Tomita-Yokotani, K., Yoshitama, K., 2008. Flavonoids in the leaves of *Oxalis corniculata* and sequestration of the flavonoids in the wing scales of the pale grass blue butterfly, *Pseudozizeeria maha*. *J. Plant Res.* 121, 133–136.
- Mohamed, E.A., Ahmed, H.I., Zaky, H.S., Badr, A.M., 2021. Sesame oil mitigates memory impairment, oxidative stress, and neurodegeneration in a rat model of Alzheimer's disease. A pivotal role of NF- $\kappa$ B/p38MAPK/BDNF/PPAR- $\gamma$  pathways. *J. Ethnopharmacol.* 267, 113468.

- Mohammed, H.A., Khan, R.A., Abdel-Hafez, A.A., Abdel-Aziz, M., Ahmed, E., Enany, S., Mahgoub, S., Al-Rugaie, O., Alsharidah, M., Aly, M.S., Mehany, A.B., 2021. Phytochemical profiling, in vitro and in silico anti-microbial and anti-cancer activity evaluations and Staph GyraseB and h-TOP-II $\beta$  receptor-docking studies of major constituents of *Zygophyllum coccineum* L. Aqueous-ethanolic extract and its subsequent fractions: an approach to validate traditional phytomedicinal knowledge. *Molecules* 26 (3), 577.
- Montibeller, L., De Belleoche, J., 2018. Amyotrophic lateral sclerosis (ALS) and Alzheimer's disease (AD) are characterized by differential activation of ER stress pathways: focus on UPR target genes. *Cell Stress Chaperones* 23, 897–912.
- Morris, R., 1984. Developments of a water-maze procedure for studying spatial learning in the rat. *J. Neurosci. Methods* 11 (1), 47–60.
- Mountaki, C., Dafnis, I., Panagopoulou, E.A., Vasilakopoulou, P.B., Karvelas, M., Chiou, A., Karathanos, V.T., Chroni, A., 2021. Mechanistic insight into the capacity of natural polar phenolic compounds to abolish Alzheimer's disease-associated pathogenic effects of apoE4 forms. *Free Radic. Biol. Med.* 171, 284–301.
- Mukherjee, S., Koley, H., Barman, S., Mitra, S., Datta, S., Ghosh, S., Paul, D., Dhar, P., 2013. *Oxalis corniculata* (Oxalidaceae) leaf extract exerts in vitro antimicrobial and in vivo anticolonizing activities against *Shigella dysenteriae* 1 (NT4907) and *Shigella flexneri* 2a (2457T) in induced diarrhea in suckling mice. *J. Med. Food* 16 (9), 801–809.
- Mukherjee, S., Pal, S., Chakraborty, R., Koley, H., Dhar, P., 2018. Biochemical assessment of extract from *Oxalis corniculata* L.: its role in food preservation, antimicrobial and antioxidative paradigms using in situ and in vitro models. *Indian J. Exp. Biol.* 56 (4), 230–243.
- Mushir, A., Jahan, N., Ashraf, N., Imran, M.K., 2015. Pharmacological and therapeutic potential of *Oxalis corniculata* Linn. *Discov. Phytomed.* 2 (3), 18–22.
- Na, H., Yang, J.B., Zhang, Z., Gan, Q., Tian, H., Rajab, I.M., Potempa, L.A., Tao, Q., Qiu, W.Q., 2023. Peripheral apolipoprotein E proteins and their binding to LRP1 antagonize Alzheimer's disease pathogenesis in the brain during peripheral chronic inflammation. *Neurobiol. Aging* 127, 54–69.
- Naseri, F., Sirati-Sabet, M., Sarlaki, F., Keimasi, M., Mokarram, P., Siri, M., Ghasemi, R., Shahsavari, Z., Goshadrou, F., 2022. The effect of ghrelin on apoptosis, necroptosis and autophagy programmed cell death pathways in the hippocampal neurons of amyloid- $\beta$  1–42-induced rat model of alzheimer's disease. *Int. J. Pept. Res. Therapeut.* 28 (5), 151.
- Ohno, M., 2018. PERK as a hub of multiple pathogenic pathways leading to memory deficits and neurodegeneration in Alzheimer's disease. *Brain Res. Bull.* 141, 72–78.
- Özener, N., Efferth, T., 2021. Phytochemical inhibitors of the NLRP3 inflammasome for the treatment of inflammatory diseases. *Pharmacol. Res.* 170, 105710.
- Pang, Y., Lin, W., Zhan, L., Zhang, J., Zhang, S., Jin, H., Zhang, H., Wang, X., Li, X., 2022. Inhibiting autophagy pathway of PI3K/AKT/mTOR promotes apoptosis in SK-N-sh cell model of alzheimer's disease. *J. Healthc. Eng.* 2022, 6069682.
- Patel, M., Singh, S., 2022. Apigenin attenuates functional and structural alterations via targeting NF-kB/Nrf2 signaling pathway in LPS-induced parkinsonism in experimental rats: apigenin attenuates LPS-induced Parkinsonism in experimental rats. *Neurotox. Res.* 40 (4), 941–960.
- Pires, M., Rego, A.C., 2023. ApoE4 and alzheimer's disease pathogenesis—mitochondrial deregulation and targeted therapeutic strategies. *Int. J. Mol. Sci.* 24 (1), 778.
- Ramesh, M., Govindaraju, T., 2022. Multipronged diagnostic and therapeutic strategies for Alzheimer's disease. *Chem. Sci.* 13 (46), 13657–13689.
- Rizvi, S.H.M., Parveen, A., Ahmad, I., Ahmad, I., Verma, A.K., Arshad, M., Mahdi, A.A., 2016. Aluminum activates PERK-eif2 $\alpha$  signaling and inflammatory proteins in human neuroblastoma SH-SY5Y cells. *Biol. Trace Elem. Res.* 172 (1), 108–119.
- Sarter, M., Bodewitz, G., Stephens, D.N., 1988. Attenuation of scopolamine-induced impairment of spontaneous alternation behaviour by antagonist but not inverse agonist and agonist  $\beta$ -carbolines. *Psychopharmacology* 94 (4), 491–495.
- Sasaguri, H., Hashimoto, S., Watamura, N., Sato, K., Takamura, R., Nagata, K., Tsubuki, S., Ohshima, T., Yoshiki, A., Sato, K., 2022. Recent advances in the modeling of Alzheimer's disease. *Front. Neurosci.* 16, 334.
- Senthil Kumar, K., 2010. B. Raj Kapoor Effect of *Oxalis corniculata* L. extracts on antioxidant enzymes levels in rat brain after induction of seizures by MES and PTZ. *Int. J. Pharm.* 1 (2), 58–61.
- Shacham, T., Patel, C., Lederkremer, G.Z., 2021. PERK pathway and neurodegenerative disease: to inhibit or to activate? *Biomolecules* 11 (3), 354.
- Sharifi-Rad, J., Quispe, C., Bouyahya, A., El Menyiy, N., El Omari, N., Shahinozaman, M., Ara Haque Ovey, M., Koirala, N., Panthi, M., Ertani, A., Nicola, S., Lapava, N., Herrera-Bravo, J., Salazar, L.A., Changan, S., Kumar, M., Calina, D., 2022a. Ethnobotany, phytochemistry, biological activities, and health-promoting effects of the genus *bulbophyllum*. *Evid. Based Complement. Alternative Med.: eCAM* 2022, 6727609.
- Sharifi-Rad, J., Rapposelli, S., Sestito, S., Herrera-Bravo, J., Arancibia-Diaz, A., Salazar, L.A., Yeskaliyeva, B., Beyatli, A., Leyva-Gómez, G., González-Contreras, C., 2022b. Multi-target mechanisms of phytochemicals in alzheimer's disease: effects on oxidative stress, neuroinflammation and protein aggregation. *J. Personalized Med.* 12 (9), 1515.
- Sharma, R., Kumari, A., 2014. Phytochemistry, pharmacology and therapeutic application of *Oxalis corniculata* Linn.—a review. *Int. J. Pharm. Sci.* 6 (3), 6–12.
- Shi, A., Shi, H., Wang, Y., Liu, X., Cheng, Y., Li, H., Zhao, H., Wang, S., Dong, L., 2018. Activation of Nrf2 pathway and inhibition of NLRP3 inflammasome activation contribute to the protective effect of chlorogenic acid on acute liver injury. *Int. immunopharmacol.* 54, 125–130.
- Shinohara, M., Tachibana, M., Kanekiyo, T., Bu, G., 2017. Thematic review series: ApoE and lipid homeostasis in alzheimer's disease: role of LRP1 in the pathogenesis of alzheimer's disease: evidence from clinical and preclinical studies. *J. Lipid Res.* 58 (7), 1267.
- Sik, B., Kapcsándi, V., Székelyhidi, R., Hanczné, E.L., Ajtony, Z., 2019. Recent advances in the analysis of rosmarinic acid from herbs in the lamiaceae family. *Nat. Prod. Commun.* 14 (7).
- Silalahi, M., 2022. Utilization of *Oxalis corniculata* Linn as a traditional medicine and its bioactivity. *Magna Scientia Adv. Res. Rev.* 5 (2), 27–33.
- Skalny, A.V., Aschner, M., Jiang, Y., Gluhcheva, Y.G., Tizabi, Y., Lobinski, R., Tinkov, A. A., 2021. Molecular mechanisms of aluminum neurotoxicity: update on adverse effects and therapeutic strategies. *Advances in neurotoxicology* 5, 1–34. Academic press, 2021.
- Soni, A., Sosa, S., 2013. Phytochemical analysis and free radical scavenging potential of herbal and medicinal plant extracts. *J. Pharmacogn. Phytochem.* 2 (4), 22–29.
- Spano, M., Di Matteo, G., Ingallina, C., Ambroselli, D., Carradori, S., Gallorini, M., Giusti, A.M., Salvo, A., Grosso, M., Mannina, L., 2022. Modulatory properties of food and nutraceutical components targeting NLRP3 inflammasome activation. *Nutrients* 14 (3), 490.
- Sun, L.C., Zhang, H.B., Gu, C.D., Guo, S.D., Li, G., Lian, R., Yao, Y., Zhang, G.Q., 2018. Protective effect of acacetin on sepsis-induced acute lung injury via its anti-inflammatory and antioxidative activity. *Arch. Pharm. Res. (Seoul)* 41, 1199–1210.
- Stancu, I.C., Lodder, C., Botella Lucena, P., Vanherle, S., Gutiérrez de Ravé, M., Terwel, D., Bottelbergs, A., Dewachter, I., 2022. The NLRP3 inflammasome modulates tau pathology and neurodegeneration in a tauopathy model. *Glia* 70 (6), 1117–1132.
- Taranalli, A., Tipare, S., Kumar, S., Torgal, S., 2004. Wound healing activity of *Oxalis corniculata* whole plant extract in rats. *Indian J. Pharmacol. Sci.* 66 (4), 444.
- Tillerson, J.L., Caudle, W.M., Reveron, M.E., Miller, G.W., 2002. Detection of behavioral impairments correlated to neurochemical deficits in mice treated with moderate doses of 1-methyl-4-phenyl-1,2,3,6-tetrahydropyridine. *Exp. Neurol.* 178, 80–90.
- Tillerson, J.L., Miller, G.W., 2003. Grid performance test to measure behavioral impairment in the MPTP-treated-mouse model of parkinsonism. *J. Neurosci. Methods* 123, 189–200.
- Turovsky, E.A., N, V., Sarimov, R.M., Simakin, A.V., Gudkov, S.V., Plotnikov, E.Y., 2022. Features of the cytoprotective effect of selenium nanoparticles on primary cortical neurons and astrocytes during oxygen–glucose deprivation and reoxygenation. *Sci. Rep.* 12 (1), 1–16.
- Tseng, C.Y., Yu, P.R., Hsu, C.C., Lin, H.H., Chen, J.H., 2023. The effect of isovitexin on lipopolysaccharide-induced renal injury and inflammation by induction of protective autophagy. *Food Chem. Toxicol.* 172, 113581.
- Verde, F., 2022. Tau proteins in blood as biomarkers of Alzheimer's disease and other proteinopathies. *J. Neural. Transm.* 129 (2), 239–259.
- Villalpando-Rodríguez, G.E., Gibson, S.B., 2021. Reactive oxygen species (ROS) regulates different types of cell death by acting as a rheostat. *Oxid. Med. Cell. Longev.* 2021.
- Villavicencio Tejo, F., Quintanilla, R.A., 2021. Contribution of the Nrf2 pathway on oxidative damage and mitochondrial failure in Parkinson and Alzheimer's disease. *Antioxidants* 10 (7), 1069.
- Wang, X., Perumalsamy, H., Kwon, H.W., Na, Y.E., Ahn, Y.J., 2015. Effects and possible mechanisms of action of acacetin on the behavior and eye morphology of *Drosophila* models of Alzheimer's disease. *Sci. Rep.* 5, 16127.
- Welcome, M.O., 2020. Blood brain barrier inflammation and potential therapeutic role of phytochemicals. *PharmaNutrition* 11, 100177.
- Yang, J., Wise, L., Fukuchi, K.-i., 2020. TLR4 cross-talk with NLRP3 inflammasome and complement signaling pathways in Alzheimer's disease. *Front. Immunol.* 11, 724.
- You, G., Yao, J., Liu, Q., Li, N., 2022. The strategies for treating "alzheimer's disease": insulin signaling may be a feasible target. *Curr. Issues Mol. Biol.* 44 (12), 6172–6188.
- Yu, T.-W., Lane, H.-Y., Lin, C.-H., 2021. Novel therapeutic approaches for alzheimer's disease: an updated review. *Int. J. Mol. Sci.* 22 (15), 8208.
- Yu, Q., Liu, M., Zhao, T., Su, M., Wang, S., Xu, W., He, S., Li, K., Mu, X., Wu, J., Sun, P., 2023. Mechanism of baixiangdan capsules on anti-neuroinflammation: combining dry and wet experiments. *Aging* 15 (15), 7689.
- Zeb, A., Imran, M., 2019. Carotenoids, pigments, phenolic composition and antioxidant activity of *Oxalis corniculata* leaves. *Food Biosci.* 32, 100472.
- Zhang, M., Yu, J., Liu, A., Liu, Q.Q., Sun, T., Li, X., Du, Y., Li, J., Wang, B., Yang, Q., 2023. Luteolin in the Qi Bi Anshen decoction improves propionic acid-induced autism-like behavior in rats by inhibiting LRP1/MMP9. *Phytomedicine* 118, 154965.
- Zhang, T., Wang, S., Niu, Q., 2019. Effect of aluminum-maltolate on the content of A $\beta$  protein and the expression of ApoER2, VLDLRs, and LRP1 in PC12-ApoE4 cells. *Neurotox. Res.* 35, 931–944.
- Zhang, Y., Zhang, P., Cheng, Y., 2008. Structural characterization of isoprenylated flavonoids from Kushen by electrospray ionization multistage tandem mass spectrometry. *J. Mass Spectrom.* 43 (10), 1421–1431.
- Zhang, W., Xu, M., Yu, C., Zhang, G., Tang, X., 2010. Simultaneous determination of vitexin-4''-O-glucoside, vitexin-2''-O-rhamnoside, rutin and vitexin from hawthorn leaves flavonoids in rat plasma by UPLC-ESI-MS/MS. *J. Chromatogr B Analyt Technol Biomed Life Sci.* 1 878 (21), 1837–1844.